STIC-ILL

Adams
20-

From: Turner, Sharon
Sent: Tuesday, June 12, 2001 8:59 AM
To: STIC-ILL
Subject: 09155076

Please Provide

Rakonczay et al., 1986 J. Neurochem. 46, 280-287

Brimijoin et al., 1993, Neuroscience 54, 201-223

Dagerlind et al., Neuroscience 54:1079-1090

Sharon L. Turner, Ph.D.
USPTO CM1-10B09
Biotechnology GAU 1647
(703) 308-0056

Article title	Death of intermediolateral spinal cord neurons follows selective, complement-mediated destruction of peripheral preganglionic sympathetic terminals by acetylcholinesterase antibodies
Article identifier	030645229300219H
Authors	Brimijoin_S Moser_V Hammond_P Oka_N Lennon_V_A
Journal title	Neuroscience
ISSN	0306-4522
Publisher	Pergamon
Year of publication	1993
Volume	54
Issue	1
Supplement	0
Page range	201-223
Number of pages	23
User name	Adonis
Cost centre	Development
PCC	$20.00
Date and time	Tuesday, June 12, 2001 9:26:22 AM

Neuroscience Vol. 54, No. 1, pp. 201–223, 1993
Printed in Great Britain

0306-4522/93 $6.00 + 0.00
Pergamon Press Ltd

DEATH OF INTERMEDIOLATERAL SPINAL CORD NEURONS FOLLOWS SELECTIVE, COMPLEMENT-MEDIATED DESTRUCTION OF PERIPHERAL PREGANGLIONIC SYMPATHETIC TERMINALS BY ACETYLCHOLINESTERASE ANTIBODIES

S. BRIMIJOIN,*† V. MOSER,‡ P. HAMMOND,* N. OKA*§ and V. A. LENNON‖

*Department of Pharmacology and ‖Departments of Neurology, Immunology, and Laboratory Medicine, Mayo Clinic, Rochester, MN 55905, U.S.A.
‡ManTech Environmental Technology Inc., Research Triangle Park, NC 27709, U.S.A.

Abstract—Systemically injected anti-acetylcholinesterase antibodies in rats cause selective lesions of preganglionic sympathetic neurons. Adult rats were examined up to four months after a single i.v. injection of murine monoclonal acetylcholinesterase antibodies or normal immunoglobulin G (1.5 mg). Within 4 h, antibody-treated rats developed ptosis, a sign of sympathetic dysfunction that was never reversed. Persistent pupillary constriction reflected preserved and unopposed parasympathetic function. Weight gain was depressed, but locomotor activity, excitability, and sensorimotor responses were normal, and gross neuromuscular performance was near normal. These findings were supported by biochemical evidence for selective sympathetic damage. Acetylcholinesterase activity was reduced for the whole period of observation in sympathetic ganglia and adrenal glands but fell only transiently in muscle and serum. At all times, choline acetyltransferase activity (a marker of presynaptic terminals) was unaffected in muscle but grossly depleted in ganglia. Light and electron microscopy showed that preganglionic sympathetic terminals of superior cervical ganglia were severely damaged while parasympathetic ganglia were less affected and motor endplates of skeletal muscle were apparently spared. Immunocytochemistry revealed punctate deposits of murine immunoglobulin G and complement component C3 in ganglionic neuropil 12 h after antibody injection. This finding was consistent with complement-mediated lysis of preganglionic terminals. Morphometric analysis of preganglionic neurons in the intermediolateral nucleus of the spinal cord showed progressive loss of cholinergic perikarya over several months.

We conclude that antibody-induced destruction of ganglionic terminals leads to death of preganglionic sympathetic neurons and, hence, permanent dysautonomia.

Cholinergic synapses in the peripheral and central nervous systems are richly endowed with acetylcholinesterase (AChE). The large oligomeric forms of AChE are anchored on the outer leaflet of nerve and muscle plasma membranes and embedded in the synaptic basal lamina of muscle.[10,19,34,57] At these exposed sites, AChE is accessible to antibodies and could be a target of autoimmunity, as are postsynaptic nicotinic acetylcholine receptors in myasthenia gravis[31,39,54] and presynaptic calcium channels in Lambert–Eaton myasthenic syndrome.[30] It is not yet known if humans develop autoimmunity to AChE. However, we have developed a passive-transfer model of such a disorder by injecting murine monoclonal AChE-antibodies into rats.[9,46] This model has many unexpected features, including similarity to human dysautonomia.

One might expect AChE-antibodies, like organophosphate anticholinesterases, to disrupt motor performance and overstimulate the parasympathetic system. In fact, AChE-antibodies cause no parasympathetic signs and little motor disability, but they rapidly impair sympathetic function and induce lowered blood pressure, reduced heart-rate, and permanent eyelid-drooping (ptosis).[9] The long-lasting autonomic disability reflects a novel form of sympathectomy, characterized by loss of preganglionic sympathetic nerve terminals with sparing of postganglionic adrenergic cells.[9] Thus far, the biochemical and structural bases of these reactions, and the extent of dysfunction, have been incompletely defined.

Among the issues remaining to be resolved are: (i) the temporal course of neurobehavioral abnormalities and their biochemical correlates; (ii) the distribution of antibody-induced lesions in different AChE-bearing tissues; (iii) the immunologic mechanism of the lesions; (iv) the factors that determine vulnerability and resistance of different cell types; and (v) the reason why lesions in the periphery should produce permanent dysfunction. We approached these issues by systematically observing neurobehavioral

†To whom correspondence should be addressed.
§Present address: Department of Neurology, Kyoto University, Kyoto, Japan.

Abbreviations: AChE, acetylcholinesterase; BuChE, butyrylcholinesterase; ChAT, choline acetyltransferase; EDTA, ethylenediaminetetra-acetate; FITC, fluorescein isothiocyanate; GFAP, glial fibrillary acidic protein; IML, intermediolateral cell column.

parameters for several months, with accompanying measurements of cholinergic marker enzymes in selected tissues. In three tissues, sympathetic ganglia, skeletal muscle, and heart, we attempted to define the structural pattern of IgG-induced lesions. To investigate immunologic mechanisms further, we followed the deposition of AChE antibodies and complement at the site of the lesions. Finally, we conducted morphometric studies of preganglionic neurons in the spinal cord.

EXPERIMENTAL PROCEDURES

Experimental animals

Male albino Sprague–Dawley rats (Harlan Sprague–Dawley, Indianapolis, IN) were purchased at age 40 days (body weight 215–235 g); a total of 178 were used in this study. Rats for neurobehavioral experiments were housed individually in plastic cages with hardwood chip bedding and *ad libitum* access to water and food (Purina Rodent Chow no. 5002); other rats were housed three to a cage in similar conditions. Ten days of habituation were allowed before behavioral testing began.

Antibody injections

Murine IgG2b monoclonal antibodies to rat brain AChE[45] (ZR 2, 3, 4, 5, and 6) were purified by chromatography on DEAE–Affigel Blue[11] (BioRad, Richmond CA). *In vitro* the antibodies bind avidly to all molecular forms of solubilized AChE from all tissues tested (including plasma, heart, sympathetic ganglia, diaphragm, extensor digitorum longus, and whole brain).[8,45] After systemic injection *in vivo*, the antibodies do not bind measurably to brain AChE,[45] probably because they are largely confined to the peripheral compartment. Each antibody recognizes a different antigenic determinant of the AChE molecule. None reacts with butyrylcholinesterase (BuChE) or interferes with AChE's catalytic activity.[45] An equal-part mixture of the antibodies (total, 1.5 mg in 2 ml 0.9% NaCl) was injected into the tail vein under light ether anesthesia. Controls received the same amount of normal mouse serum IgG (PelFreez Biologicals, Rogers, AK).

Nerve crush lesions

For comparison with antibody-induced nerve damage, we also tested the effects of simple mechanical injury. Under ether anesthesia, the preganglionic sympathetic chain on the right side was exposed in its course along the common carotid artery by gentle dissection with scissors and a blunt forceps. The nerve was then crushed approximately 1 cm proximal to the superior cervical ganglion by 15 s of pressure applied with a sterile watchmaker's forceps. Skin incisions were sutured, and recovery was uneventful.

Neurobehavioral tests

Neurologic integrity was assessed by an experienced observer administering a standard series of repeated neurobehavioral tests (a "functional observational battery") and an automated measure of motor activity. Full details of the procedures and the scoring criteria have been published.[36,37] Observations in the home cage included posture and involuntary movements. Lacrimation, salivation, palpebral closure, piloerection, ease of removal, and response to handling were scored as the rat was removed from the cage. The rat was then placed in an open field to score gait abnormalities, arousal, mobility, and clonic or tonic movements. Rearing, urination, and defecation were counted over a 3-min period. Reactions to an approach, touch, click and tail-pinch were rated, and the aerial righting reflex and the pupillary response to light were tested. Finally, fore- and hindlimb grip-strength, landing foot-splay, core-temperature, and weight were measured. All subjective measures were ranked by standardized scoring criteria; continuous measures were quantified objectively with appropriate devices.[36,37] Between 10 and 45 min after the functional observations were completed, each rat was placed in a figure-of-eight maze to record motor activity as photobeam interruptions over a 60-min session. Baseline values for all measures were obtained the day before IgG injection (time 0); the tests were repeated, three, nine, 24, 45, 73, and 94 days after injection.

Tissue samples and enzyme assays

For biochemical studies, rats were killed by an overdose of ether or pentobarbital at one, seven, 30 and 113 days after injection. Blood was drawn from the heart, and the animals were exsanguinated by aortic perfusion with approximately 300 ml of 0.9% NaCl. The following tissues were collected on ice and frozen at −20°C until assay (usually within two weeks): superior cervical ganglia, stellate ganglia, adrenal glands, left hemidiaphragm, hearts, brains, and tails.

Choline acetyltransferase (ChAT) activity was measured by Fonnum's method,[20] with choline-free blank samples. Tissues were homogenized in 10 mM EDTA, pH 7.4, with 0.5% Triton X-100, and 0.2% bovine serum albumin. Immunoprecipitations with a specific monoclonal antibody to ChAT (Boehringer–Mannheim, Indianapolis, IN) were carried out to control for interference by carnitine acetyltransferase. Over 75% of the activity in heart, and over 95% in whole brain, ganglia, or diaphragm reflected authentic ChAT that selectively bound to antibody.

AChE activity was measured spectrophotometrically[18] or, in density gradients, radiometrically.[27] Tissues were homogenized in 0.05 M sodium phosphate buffer, pH 7.4, with 1% Triton X-100 and 0.5 M NaCl. Ethopropazine (10^{-4} M) was added to all samples to inhibit BuChE.

Analysis of acetylcholinesterase molecular forms and acetylcholine receptors

For analysis of AChE forms, the homogenization buffer (above) was supplemented with antiproteases: pepstatin, 3×10^{-5} M, and leupeptin, 5×10^{-5} M. AChE forms in extracts of diaphragm were separated by ultracentrifugation (17 h, 34,000 r.p.m.) on 5-ml 5–20% sucrose density gradients containing 0.5% Triton X-100, 0.5 M NaCl, 0.2 mM EDTA, and 0.05 M Tris–HCl buffer, pH 7.4. To remove IgG-bound AChE, duplicate tissue extracts were first incubated (2 h, 23°C) with rabbit anti-mouse IgG coupled to a solid phase (Pansorbin, Calbiochem–Behring, La Jolla, CA). In both cases, gradient fractions collected sequentially from the bottom were assayed for AChE activity. Catalase (11.3S) was the sedimentation marker. Relative proportions of each molecular form were calculated from the sedimentation profile of AChE activity.

To quantitate nicotinic acetylcholine receptors in muscle, skinned tail tissue was homogenized twice in 0.01 M sodium phosphate pH 7.3, with 0.1 M NaCl, 0.02% NaN_3, 0.001 M EDTA. Receptors extracted from pelleted tissue in the same buffer containing 2% Triton X-100 were measured by immunoprecipitation of [^{125}I]α-bungarotoxin binding sites.[35]

Antibody detection

Murine immunoglobulins in rat serum were measured with a specific two-site enzyme-linked immunosorbent assay,[8] based on rat anti-mouse IgG (Boehringer–Mannheim). AChE-containing immune complexes extracted from tissues were measured in terms of AChE activity selectively adsorbed by solid-phase rabbit anti-mouse IgG.[8]

Acetylcholinesterase histochemistry

Ganglia and adrenals were collected after perfusion through the ascending aorta with 300 ml of 0.9% NaCl followed by 200 ml of 4% phosphate-buffered formalin,

pH 7.4; the tissues were postfixed *in vitro* for 24 h and then were cryoprotected by incubation for 16–40 h in 15% sucrose. Skeletal and cardiac muscle retained better morphology when the perfusion was omitted. Therefore, immediately upon induction of surgical anesthesia, muscles and hearts were removed and snap-frozen in acetone–dry-ice for 15 min; frozen tissues were then directly mounted in the cryostat.

AChE-histochemistry was conducted on cryostat sections (15–20 μm), as described by Koelle and Friedenwald[29] or Tago *et al.*[53] Slide-mounted sections were incubated in ethopropazine (10^{-4} M, 1 h) to inactivate BuChE before substrate was added (acetylthiocholine, 2–4 mM). Control sections were preincubated as well with BW284C51, 10^{-5} M, to demonstrate reaction specificity. Stained slides were dried overnight at 37°C and coverslipped in Permount.

Choline acetyltransferase and glial fibrillary acidic protein immunocytochemistry

Spinal cords were fixed *in situ* by perfusion through the ascending aorta with 200 ml of 4% buffered formalin–0.2% picric acid. The tissue was postfixed for 1 h in the same solution and cryoprotected with 15% sucrose for 48 h. ChAT was stained immunohistochemically in 20-μm cryostat sections with a monoclonal rat anti-ChAT antibody[17] (see above), diluted to 5 μg/ml. Bound antibody was visualized by biotinylated anti-rat IgG and avidin–biotin–peroxidase (Vector Labs) according to Hsu *et al.*[25] Glial fibrillary acidic protein (GFAP) was stained with a specific mouse monoclonal antibody (5 μg/ml; Boehringer–Mannheim) followed by biotinylated rat anti-mouse IgG and avidin–biotin–peroxidase. Control sections were treated with appropriate normal sera or with no first antibody. "Nissl substance" was stained with thionin according to the method of Donovick.[16]

IgG and complement immunocytochemistry

Samples were from rats injected 12 h earlier with anti-AChE antibodies or normal mouse IgG. All tissues were snap-frozen in dry-ice–acetone without prior perfusion. To remove nonspecifically adsorbed IgG, slide-mounted sections (16 μm) were rinsed 3 × 10 min in phosphate-buffered saline solution. Tissue-bound IgG was stained with goat anti-mouse-IgG (1:15 dilution; Boehringer–Mannheim Biochemicals, Indianapolis, IN) conjugated with fluorescein isothiocyanate (FITC). This antibody cross-reacted poorly with rat IgG and avoided background staining of host immunoglobulin. Some sections were processed by the "ABC" method of Hsu *et al.*,[25] using biotinylated horse anti-mouse IgG and avidin–biotin–peroxidase (Vector Labs).

Immunoreactive complement component-C3 was stained with a goat antiserum (1:300 dilution; Quidel, San Diego, CA); control slides were prepared with normal goat serum at the same dilution. FITC-labeled monoclonal anti-goat IgG (Boehringer–Mannheim) was selected as second antibody after tests proved that it did not recognize murine IgG and gave no false signals from the previously injected anti-AChE IgG. To reveal nicotinic acetylcholine receptors in addition to complement, rhodamine-conjugated α-bungarotoxin (1:1000 dilution; Molecular Probes, Eugene, OR) was applied with the second antibody. Trials with single staining showed no crossover of fluorescence between different filter sets in the fluorescence microscope. Because the rhodamine staining was faint, the Tri-X negatives were enhanced by video processing on a Zeiss IBAS system, maintaining identical parameters throughout. Enhanced images were photographed from the video monitor.

Electron microscopy

Rats were perfused with 300 ml of isotonic NaCl followed by 300 ml of 4% formalin–2.5% glutaraldehyde in 50 mM phosphate buffer, pH 7.4. Ganglia were transferred to concentrated fixative (8% formalin, 5% glutaraldehyde) *in vitro* for a total of 1 h. They were postfixed in osmium tetroxide, dehydrated in graded alcohols, and embedded in EPON–araldite. Thick sections (1 μm) were Nissl-stained with Toluidine Blue.[28] Thin sections stained with uranyl acetate and lead citrate were examined and photographed on a JEOL 1200 electron microscope.

AChE histochemistry at the ultrastructural level was performed as described by Tago *et al.*,[53] omitting cobalt intensification. After fixation but before dehydration and embedding (see above), endplate-rich slices (< 1 mm) from extensor digitorum longus muscle were reacted with acetylthiocholine substrate (1.8 mM, 120 min). BuChE was inactivated by pre-incubation with ethopropazine. Subsequently the specimens were processed as for conventional electron microscopy.

Morphometry

Morphometric studies of spinal cord emphasized the intermediolateral cell column (IML). The IML was unmistakable in ChAT stains; in Nissl stains it was defined as the zone of gray matter beginning 200 μm dorsal and 300 μm lateral to the central canal, and extending another 200 μm dorsally and laterally. ChAT-positive and Nissl-stained neurons were counted in coded samples (only nucleated cells ≥ 5 μm in diameter were included); the observer was not aware of the treatment group. Thirty serial sections were taken from each spinal cord, starting at the T1–T2 intervertebral space, where preganglionic neurons to the superior cervical ganglion are most abundant[47,52] (samples were not taken from brainstem or other regions containing preganglionic parasympathetic neurons). To avoid duplications, every third section was counted (intervening gap 40 μm). The total length of cord surveyed was 600 μm, roughly twice the average distance between "nests" of preganglionic sympathetic neurons in the IML.[5,47]

Superior cervical ganglia were analysed morphometrically at the electron microscope level to estimate the frequency of cholinergic synapses and degenerating nerve fibers. Synapses were identified as characteristic synaptic triads: abutting neural processes filled with small clear vesicles and separated by distinct junctional densities. Mean frequency (number/mm^2) was determined from complete counts in three to six randomly selected grid squares from each ganglion. At least 300 nerve fibers and terminals in the same fields were also examined for signs of degeneration (electron-lucent swelling, loss of internal structure, or collapsed, electron-dense appearance).

Statistical analysis

Standard errors of the mean were the uniform measure of variation. Differences between means in multiple comparisons were evaluated by one- and two-factor analysis of variance (ANOVA). When overall effects of treatment were significant for a given measure, univariates were examined by two-tailed t-tests. Individual neurobehavioral measures were analysed as described by Moser.[36] Two-way ANOVAs used treatment as a grouping factor, and repeated measures across time. Continuous data were analysed by a linear model (GLM) with each rat's time-0 values as a covariate; rank data were analysed by a categorical procedure (CATMOD). P-values ≤ 0.05 were considered significant.

RESULTS

Neurobehavioral observations

Nine rats were given i.v. injections of anti-AChE IgG, 1.5 mg, while 10 control rats received the same amount of normal mouse IgG. The latter group exhibited no significant reactions. Rats injected with

AChE-antibody, however, developed within 30 min transient piloerection, exophthalmos, and mouth smacking, followed within 4 h by conspicuous ptosis. Another sign of sympathetic dysfunction, miosis, was noted at three days; this precluded observable responses of the pupils to light. Ptosis lasted for the whole 94-day period of observation, but miosis diminished sufficiently for pupillary reflexes to be detectable in half the antibody-treated rats at 45 days. Autonomic measures of parasympathetic function (lacrimation, salivation, urination and defecation) were always normal. Excitability, motor activity, and most indices of neuromuscular function were also unaffected, except for grip strength.

Measures of forelimb grip strength revealed a small overall difference from control (treatment effect, $P < 0.03$) without significant differences at any individual time point (Fig. 1B). Hindlimb grip was slightly weak at the first test after antibody injection and did not increase as much thereafter as in the controls (Fig. 1A), but the relative weakness was not statistically significant (treatment effect, $P = 0.056$). Taken together, the data indicate that grip strength was slightly impaired by AChE antibody, primarily in the first three weeks.

Sensorimotor tests remained largely normal, although response to light touch was increased in half of the sessions. Mild hypothermia (about 0.3°C) appeared transiently, three days after injection. Antibody-treated rats gained weight more slowly than the controls. Mean weights were reduced significantly from day 45 onwards, and were 9% below control at the last weighing ($P < 0.05$).

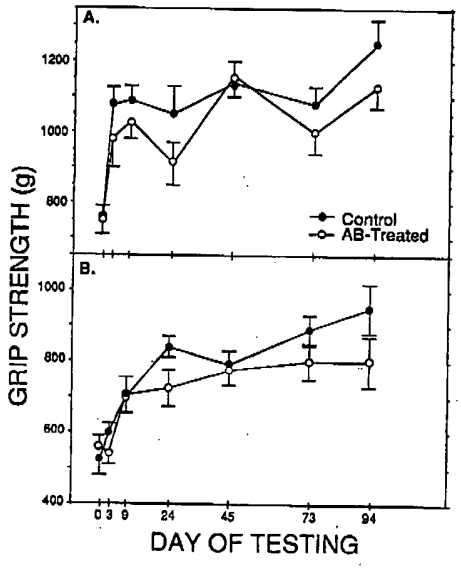

Fig. 1. Effect of AChE-antibodies on grip strength. On day 0, 10 control rats received 1.5 mg of normal mouse IgG via the tail vein, and nine antibody-treated (AB-Treated) rats received 1.5 mg of anti-AChE IgG. Maximal force of grip (average of two tests) was measured by strain gauge (means ± S.E.M. are shown). (A) Hindlimb; (B) forelimb.

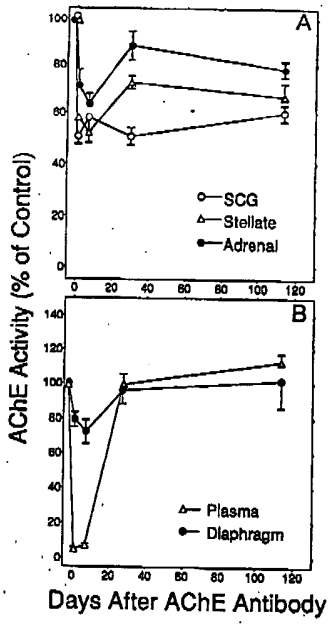

Fig. 2. Antibody-induced losses of tissue AChE. Total AChE activity from rats given anti-AChE IgG (1.5 mg, i.v.) is expressed as a percentage of the mean value in tissues harvested simultaneously from control rats injected at the same time with normal mouse IgG. Data (means ± S.E.M.) are for eight to 12 rats at each time. (A) Sympathoadrenal tissues (SCG, superior cervical ganglion) show persistent depletion of AChE. (B) Muscle and plasma show transient depletion of AChE. Note the rapid drop in the first 24 h.

Biochemical markers

At the end of the neurobehavioral experiment, 113 days (four months) after antibody injection, plasma, superior cervical and stellate ganglia, adrenal gland, right hemidiaphragm, and brain were collected for assay of AChE and ChAT. To define the time-course of biochemical changes, additional rats (four to six per group) were killed one day, one week, and one month after injection of AChE antibody or normal mouse IgG.

In the first week after antibody treatment, most tissues lost 30–40% of their AChE activity and plasma lost over 90% (Fig. 2), but brain AChE was unaffected (not illustrated). This pattern of changes echoed the distribution of immune complexes found by assays of IgG-bound enzyme (see Experimental Procedures). Much of the AChE activity in diaphragm and superior cervical ganglion was bound to antibody (45 and 22%, respectively). Less than 2% of the enzyme in brain and spinal cord was IgG-bound.

Larger oligomeric forms of muscle AChE were selectively affected, as shown by sucrose density gradient centrifugation (Fig. 3). One week after antibody-treatment, 10S and 16S AChE activities were greatly reduced, while 4S enzyme was spared. Effects on the synapse-specific 16S form were particularly strong. No 16S AChE extracted from diaphragm or other skeletal muscle was free of IgG. Similar effects on oligomeric AChE were seen in extracts of superior

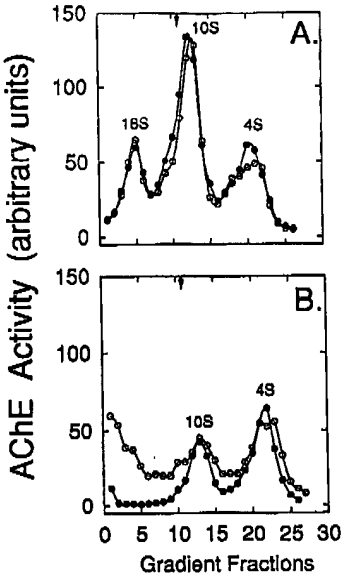

Fig. 3. Selective complexation of oligomeric AChE in muscle. Control rat (A) received normal mouse IgG; experimental rat (B) received anti-AChE IgG. Three days later, diaphragm extracts were ultracentrifuged on sucrose density gradients. AChE activities were measured in fractions collected from the bottom. Open circles: extracts applied directly to gradient; closed circles: extracts pretreated to remove IgG-bound AChE (see Experimental Procedures). Arrow shows position of sedimentation marker (catalase, 11.3S). The deficit of free oligomeric AChE in the experimental muscle may reflect a combination of IgG-complexation and enzyme depletion.

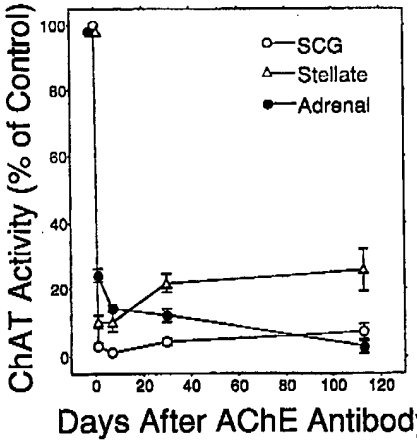

Fig. 4. Antibody-induced losses of sympathoadrenal ChAT. Total ChAT activity (a marker of cholinergic cytoplasm) from rats given anti-AChE IgG (1.5 mg, i.v.) is expressed as a percentage of the mean value in tissues harvested simultaneously from control rats given normal mouse IgG at the same time. Data (means ± S.E.M.) are for eight to 12 rats at each time. Note the rapid drop in first 24 h.

cervical ganglia (data not shown). However, the relatively small decrease in total AChE activity suggests that some oligomeric AChE persisted at motor endplates, despite complexation with IgG (Table 1). In contrast with AChE, the nicotinic acetylcholine receptors of muscle showed no changes after antibody-treatment (Table 1).

Depletion of AChE was transient in plasma and muscle but appeared to be permanent in adrenals and superior cervical ganglia (Fig. 2). In relation to age-matched controls, the deficits of ganglionic AChE activity at four months were quite similar to those at one week. In comparison, plasma AChE activity had fully recovered one month after treatment. At that time murine IgG had been cleared from the circulation, IgG–AChE complexes had disappeared from the tissues, and AChE molecular forms had reverted to the normal pattern in the diaphragm (not shown).

The presynaptic cholinergic marker, ChAT, was affected more selectively. Ganglia and adrenals showed long-lasting depletion of ChAT, even greater than the loss of AChE (Fig. 4). Superior cervical ganglia had virtually no ChAT activity during the entire four month period after injection of AChE-antibody. Stellate ganglia were less affected, but their ChAT activity never exceeded 25% of control. Adrenal ChAT was moderately depleted at one day and declined thereafter to unmeasurable levels. On the other hand, ChAT in diaphragm showed no changes after antibody-treatment, either early or late. Heart ChAT also was unaffected by AChE-antibody (data not shown).

Morphology of antibody lesions

Sympathetic ganglia, parasympathetic ganglia and cardiac muscle, and motor endplates in skeletal muscle were examined histologically to map the pattern of lesions induced by AChE-antibodies.

Table 1. Antibody effects on acetylcholinesterase molecular forms and acetylcholine receptor in muscle

		AChE Activities[a]					ACh Receptor[b]
		Unfractionated		Molecular forms			(α-bungarotoxin sites)
Group	*n*	Total	IgG-bound	4S	10S	16S	
Normal IgG	8	590 ± 38	<5%	130 ± 13	205 ± 19	110 ± 6	548 ± 29
Anti-AChE IgG	4	440 ± 36	45 ± 8%[d]	115 ± 17	73 ± 12[c]	5 ± 1[e]	497 ± 30

AChE molecular forms were extracted from left hemidiaphragm, separated by ultracentrifugation on sucrose density gradients, and assayed radiometrically; ACh receptors were extracted from tail muscle and assayed by immunoprecipitation of bound [^{125}I]α-bungarotoxin. Data are means ± S.E.M. Rats were injected one week earlier with a mixture of IgG antibodies to rat brain AChE (ZR2-6, 0.3 mg each) or normal mouse serum IgG (1.5 mg).

[a]nmol/min per hemidiaphragm; [b]fmol/gm; [c]$P < 0.05$; [d]$P < 0.005$; [e]$P < 0.0005$.

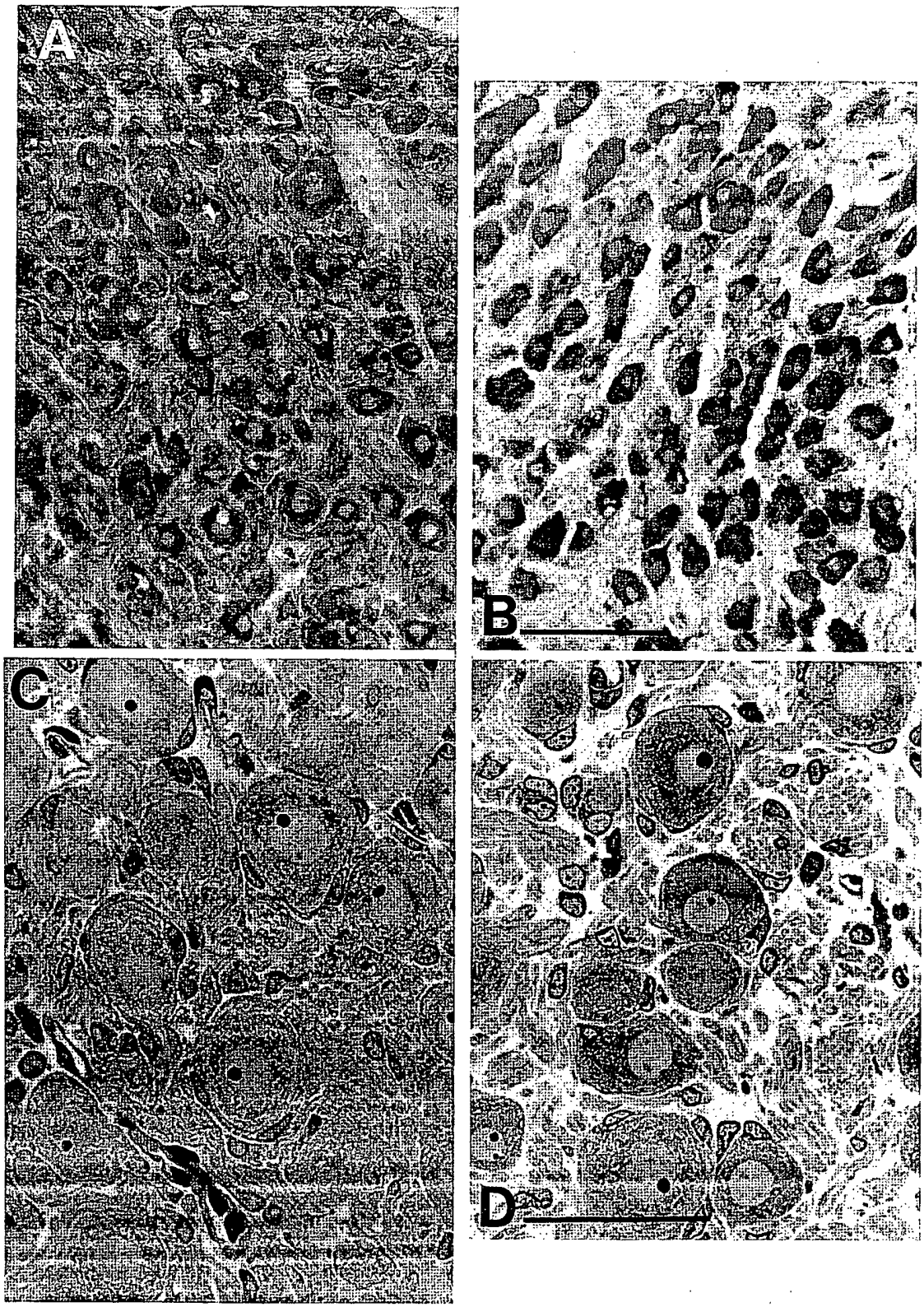

Fig. 5. Top: loss of AChE staining in ganglionic neuropil. Rats were given normal mouse serum IgG (A) or anti-AChE IgG (B), 1.5 mg/kg, i.v. Five days later, superior cervical ganglia were formalin-fixed, and frozen sections (18 μm) were stained for AChE activity by the method of Tago *et al.*[53] Scale bar = 100 μm. Bottom: Nissl-stains. Superior cervical ganglia from identically treated rats were fixed in glutaraldehyde, embedded in Epon–Araldite, sectioned (1 μm) and stained with Toluidine Blue. Control ganglion (C) has densely packed neuropil. Experimental ganglion (D) has normal looking neurons but edematous or empty neuropil. Scale bar = 50 μm.

Sympathetic ganglia. AChE histochemistry was used to test the effects of antibodies on AChE-bearing structures in the superior cervical ganglion, one, five, seven and 90 days after i.v. injection of anti-AChE IgG (one or two rats each). At all these times, selective presynaptic damage was observed as a disappearance of AChE-reactive fibers in the neuropil, with preservation of AChE-reactive nerve cell bodies (Fig. 5A, B). Nissl stains were also made 4, 6, 12, 16, 24 h, five and 10 days after injection (one to three rats at each time). The results confirmed that postganglionic neurons survived (Fig. 5C, D). The ganglionic neuropil, however, appeared partly empty, possibly edematous, especially at five days after antibody administration. Despite this indication of fiber loss, there was little sign of a cellular inflammatory response, and mononuclear infiltrates were not seen.

Many of the superior cervical ganglia taken for light microscopy were also studied by transmission electron microscopy. Cell bodies exhibited minimal damage. Early on, the nuclear envelope was sometimes wrinkled, but vacuoles, swollen mitochondria, and other signs of cytopathology were rare (not shown). In comparison, abnormalities in ganglionic synapses were obvious (Fig. 6). Synapses counted in four control ganglia (see Experimental Procedures) showed an apparent abundance of 580 ± 160 per mm^2. The synapses deteriorated rapidly after injection of anti-AChE IgG (Fig. 6B–E). In the case examined at 4 h, when severe ptosis pointed to failing ganglionic transmission, a few normal synaptic triads still remained. Later they became scarce or absent, giving way to swollen electron-lucent profiles with indistinct junctional densities, multivesicular bodies and other cytoplasmic inclusions. In five ganglia sampled 4–24 h after treatment, neural processes with one or more such features comprised $14.4 \pm 2.3\%$ of the total vs $4.9 \pm 1.2\%$ in four controls ($P < 0.01$). After five days, no normal synapses were noted in an exhaustive review of three ganglia, three sections each (example in Fig. 6F). Overall, the ultrastructural pathology was consistent with survival of postganglionic neurons but rapid lysis and destruction of preganglionic terminals.

The ganglia taken within 24 h after antibody treatment harbored a few polymorphonuclear leucocytes and cells resembling activated macrophages (Fig. 7). Macrophages were fairly common by day 5 (~ 75/mm^2); but infiltrates of lymphocytes were never apparent. In short, there was no morphologic sign of a vigorous, cellular immune response.

Skeletal muscle and heart. Synaptic abnormalities in skeletal muscle were much less marked. Diaphragms collected one week after antibody injection showed many AChE-positive motor endplates by light microscopy (Fig. 8). Cross-sections of the central, endplate-rich region averaged 9.1 ± 1 endplates per mm^2 vs 8.8 ± 0.3 per mm^2 in controls (three rats per group). While endplate staining was strong in antibody-treated rats, relative deficits of AChE activity could be demonstrated by shortening the incubation with substrate or adding a dilute AChE-inhibitor (not shown). As in ganglia, no lymphocytic invasion was evident in the synapses. At the ultrastructural level, muscle endplates from the same antibody-treated animals exhibited typical junctional folds darkly outlined with AChE reaction product (Fig. 9). Motor neurons also appeared to be intact. Thus, the neuromuscular junction underwent little or no structural deterioration after the binding of AChE-antibody.

Cholinergic structures of the heart ranked between skeletal muscle and sympathetic ganglia in their vulnerability to AChE-antibodies. Parasympathetic ganglia of the inter-atrial septum retained numerous AChE-positive cell bodies in two rats studied one week after antibody injection (Fig. 10). Some loss of AChE was suggested by a reduced density of reaction product in the ganglionic neuropil (Fig. 10). But fibrous staining in the neuropil was still apparent, implying that many neuronal processes survived along with the ganglion cells. It could not be determined whether the surviving fibers were pre- or postganglionic. Furthermore, the data did not permit a quantitative analysis of the number and density of fibers or ganglion cells. However, qualitatively normal fiber-staining in the atrial muscle (Fig. 11) suggested that postganglionic terminals were not greatly damaged. Altogether, the histochemical results showed that cardiac neurons were at least partly resistant to the immunologic lesions.

Immunologic mechanisms

To investigate the mechanism of selective, antibody-mediated damage to sympathetic ganglia, we assessed the tissue uptake of murine IgG. Immunofluorescence cytochemistry of superior cervical ganglia from three rats examined 12 h after systemic injection of AChE-antibody showed crisp, punctate deposits of IgG (Fig. 12B). Intense spots of specific fluorescence were localized in the neuropil and around the borders of principal neurons throughout the ganglion. Ganglia from three control rats given normal mouse IgG stained dimly and diffusely in comparison.

Because the AChE-antibodies can activate complement,[9] we examined the same ganglia for deposits of the third proteolytic component, C3, which is common to the classical and alternative complement pathways. Like murine anti-AChE IgG, C3 was localized by immunofluorescence as punctate staining around large neurons and along fiber bundles in superior cervical ganglia (Fig. 12D). These abnormal deposits were unique to the three rats given AChE-antibody. No specific C3 immunoreactivity was seen in the three control specimens.

In the same animals we also tested the access of circulating IgG and the activation of complement in skeletal muscle, a "resistant tissue". Motor endplates in diaphragms of control rats did not accumulate

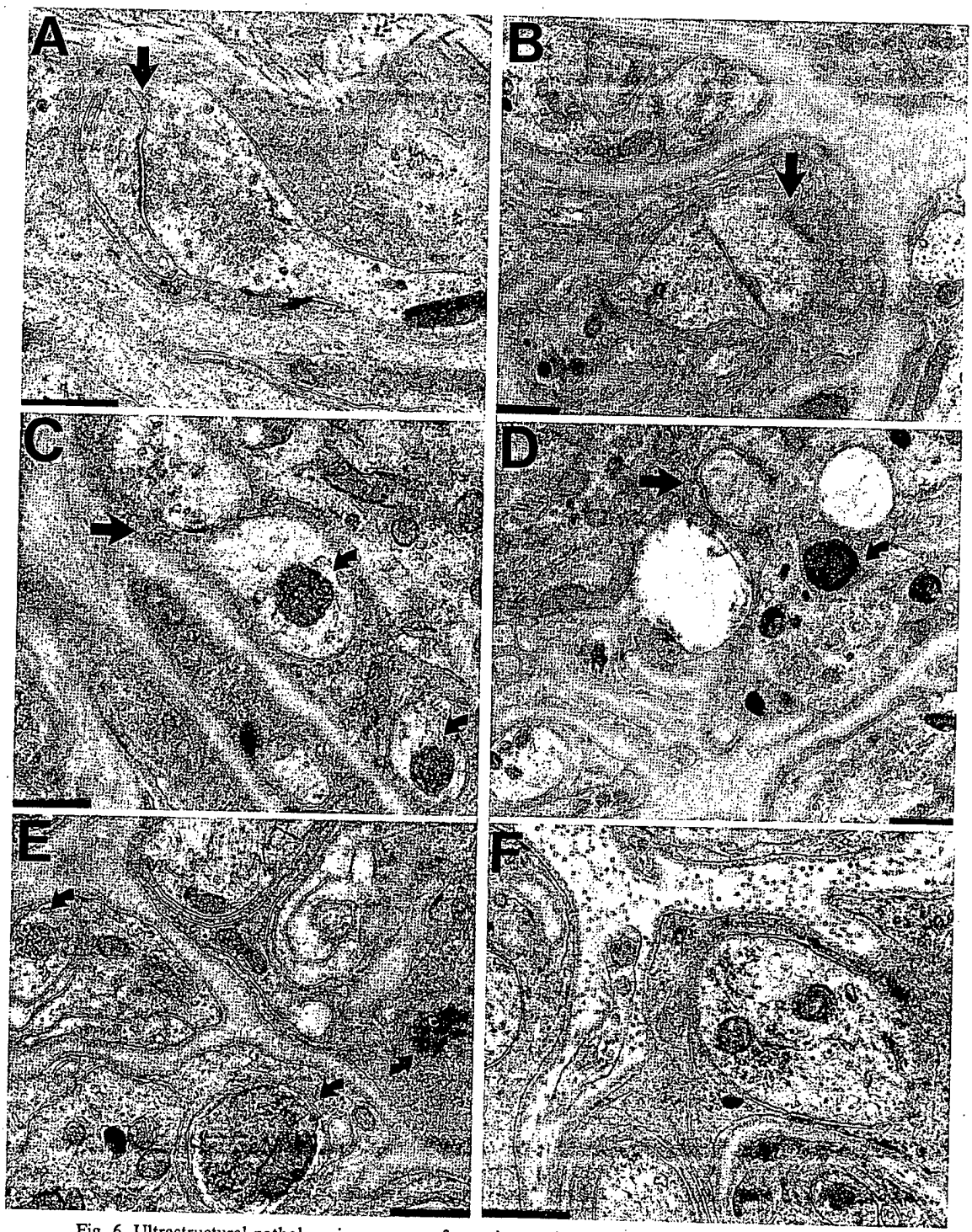

Fig. 6. Ultrastructural pathology in synapses of superior cervical ganglion. Rats were injected i.v. with 1.5 mg of normal mouse serum IgG (A) or anti-AChE IgG (B–F). Ganglia were removed at the following times: (A) 24 h; (B) 4 h; (C) 12 h; (D, E) 16 h; (F) five days. Straight arrows indicate synaptic triads. Curved arrows indicate multivesicular bodies. Scale bars = 0.5 μm.

normal mouse IgG, but the endplates of experimental rats were full of anti-AChE IgG, revealed by immunoperoxidase-staining (Fig. 13) and by immunofluorescence (not shown). These results confirmed both the access and the specific binding of antibodies to junctional AChE.

Bound AChE-antibody might not trigger immunologic lesions if it did not activate complement.

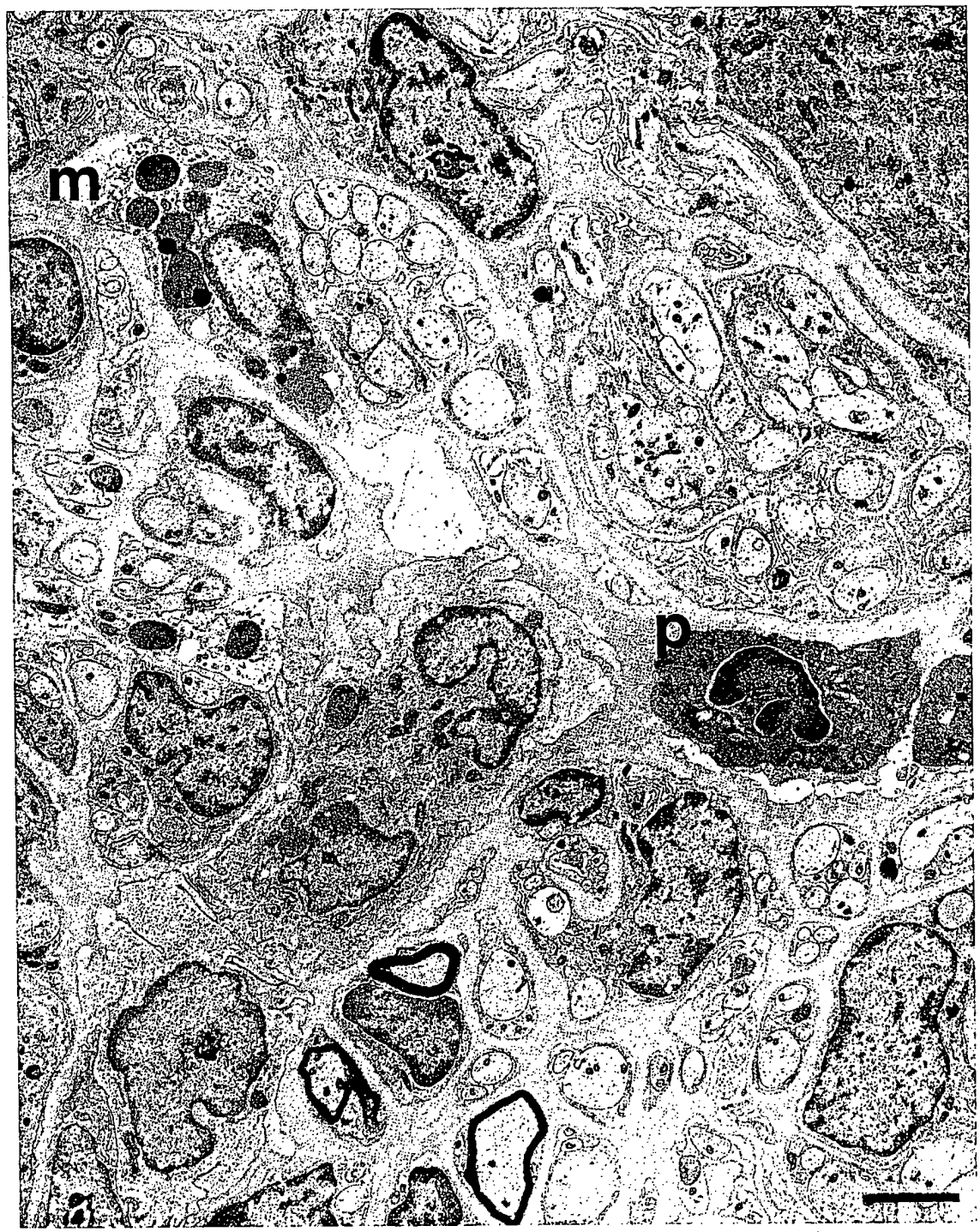

Fig. 7. Occasional inflammatory cells in superior cervical ganglion of a rat injected 16 h earlier with anti-AChE IgG. A polymorphonuclear leucocyte (p) with its characteristic multilobed nucleus, and an activated macrophage (m) with large filled and empty vacuoles are seen. Scale bar = 2 μm.

However complement activation did occur in skeletal muscle: a brilliant overlay of C3-immunofluorescence was found to colocalize with rhodamine-conjugated α-bungarotoxin in the motor endplates of the diaphragm. Every endplate labeled by the receptor probe was labeled by C3-immunofluorescence, and vice versa, yielding identical spatial patterns (Fig. 14).

Evidence for antibody binding and complement activation was obtained in cardiac tissue as well. Thus 12 h after antibody injection, striking deposits of murine IgG and C3-immunoreactivity appeared in intramural ganglia of the atrial septum and on nerve

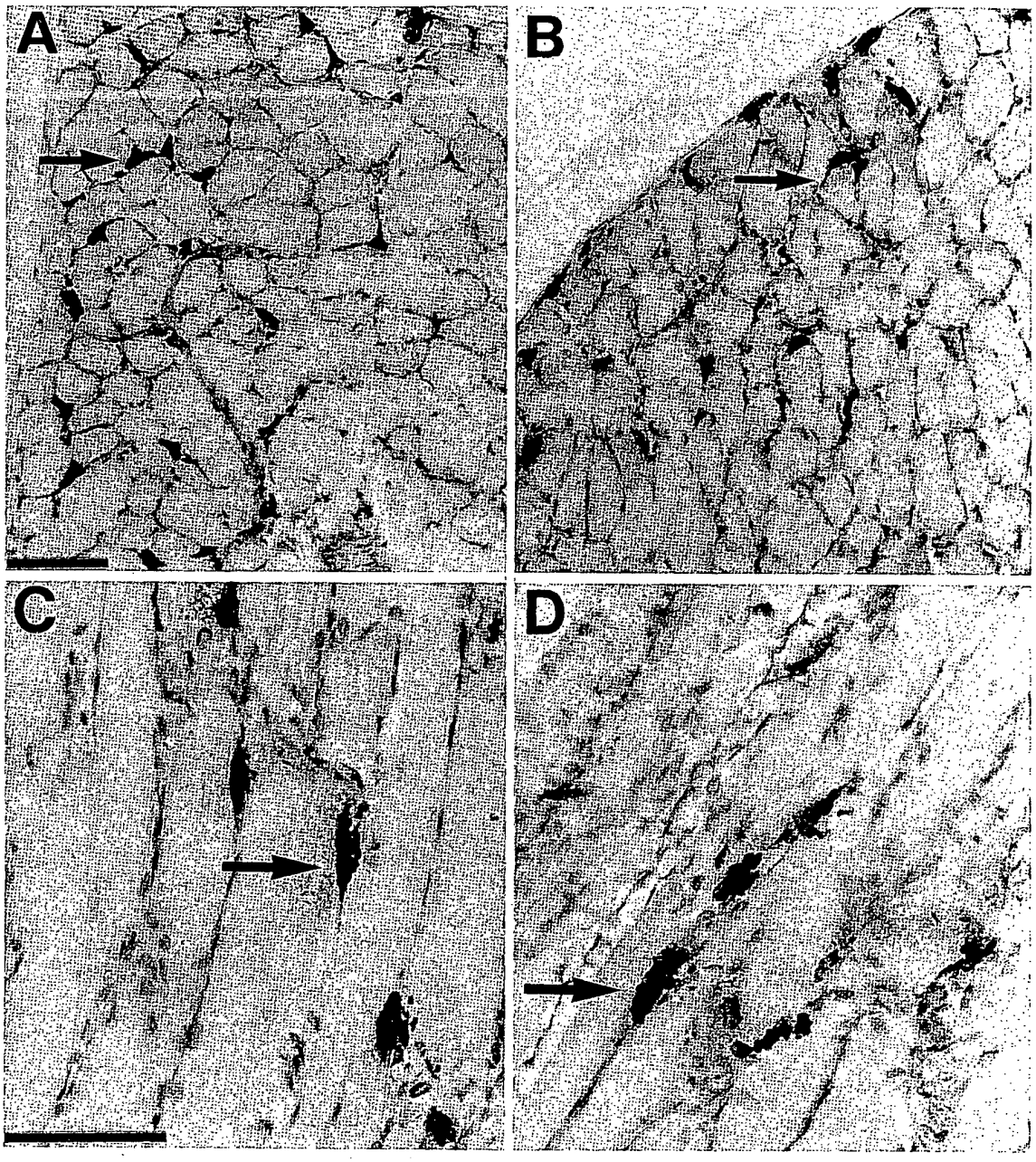

Fig. 8. Persistence of motor endplates in diaphragm. (A, C) Control rat, one week after i.v. injection of normal mouse IgG. (B, D) Experimental rat, one week after injection of anti-AChE IgG. Above, cross-sections; below, tangential sections. Samples were processed for AChE activity by the method of Koelle and Friedenwald.[29] Note generally similar frequency of intensely AChE positive endplates (arrows). Scale bars = 100 μm.

terminals in the atrial musculature (not shown). We concluded that most cholinergic synapses in the peripheral nervous system were accessible to AChE antibodies.

Comparison with nerve crush

To gain perspective on the long-lasting antibody-induced damage to preganglionic sympathetic nerves, we also assessed the recovery from simple mechanical injury of the right, mid-cervical sympathetic chain. As an index of the loss and return of preganglionic terminals, ChAT activity was measured one or six weeks later in the right and left superior cervical ganglia (three rats per group). Three unoperated rats served as controls. At one week, all operated rats showed severe unilateral ptosis, and their lesioned ganglia had no detectable ChAT activity. Ptosis lasted for three to four weeks but subsided completely

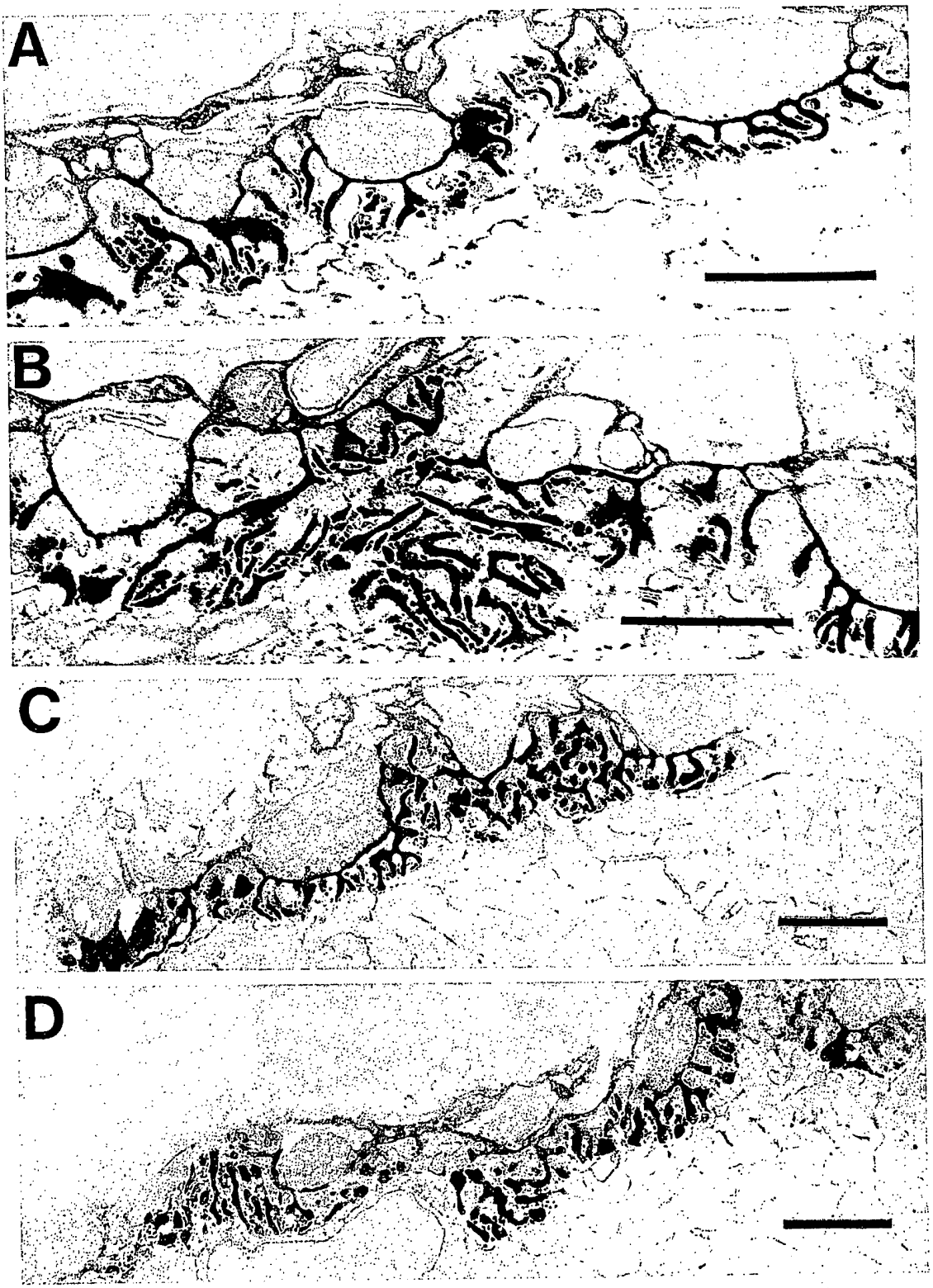

Fig. 9. Preservation of motor endplate fine structure. Synaptic AChE was stained by the method of Tago *et al.*,[53] one week after i.v. injection of normal mouse IgG (A, B; two rats) or anti-AChE IgG (C, D; two rats). Note essentially normal postjunctional folds and AChE-staining in synaptic cleft. Scale bars = 2 μm.

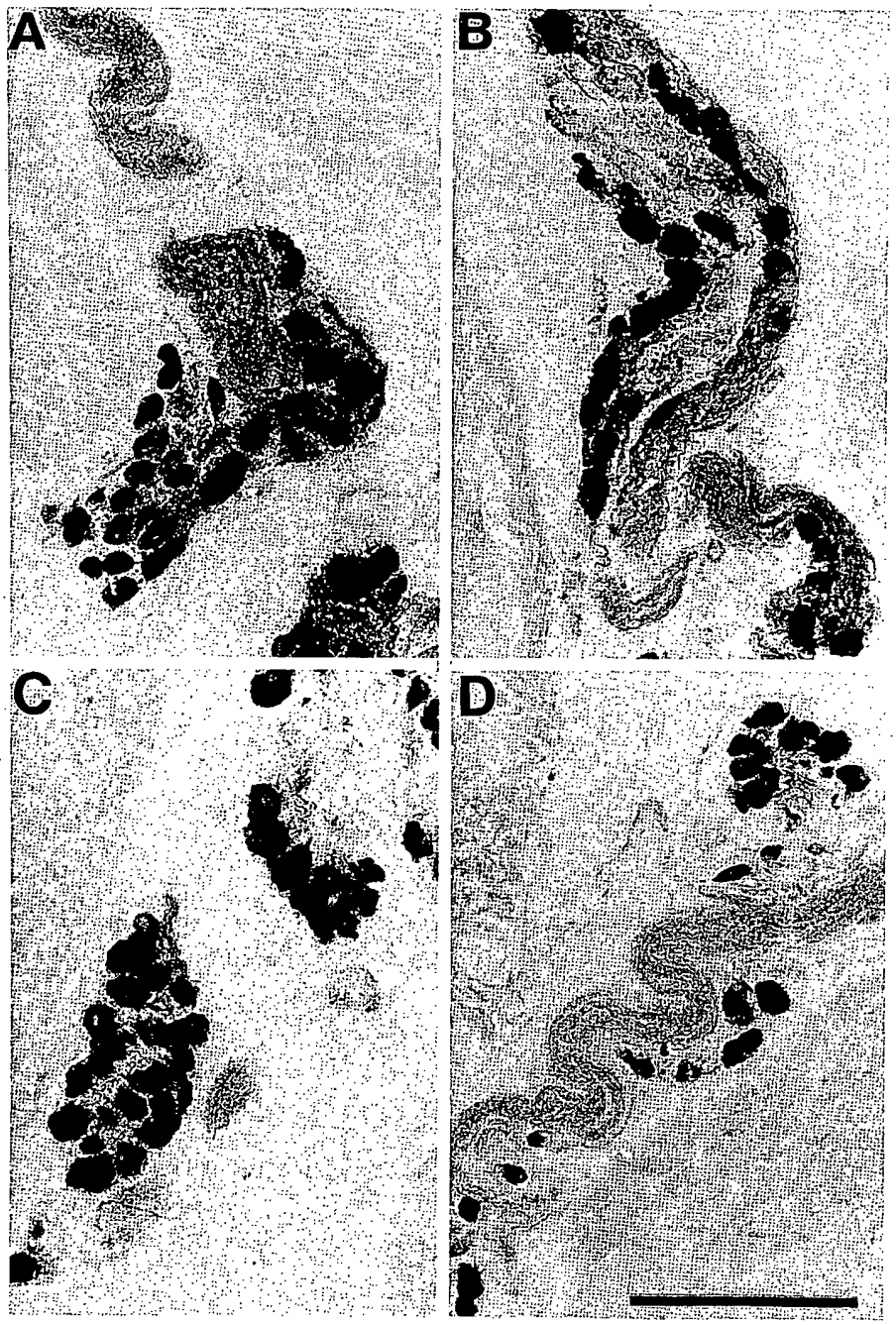

Fig. 10. Relative resistance of parasympathetic atrial ganglia to AChE IgG. Sections of inter-atrial septum were processed for AChE histochemistry. (A, B) Two control rats one week after i.v. injection of normal mouse IgG. (C, D) Two rats one week after i.v. injection of anti-AChE IgG. Intensely AChE-positive cell bodies are retained; fibrous staining in neuropil is reduced but still evident. Scale bar = 200 μm (all panels).

by six weeks. Although ganglionic ChAT activity on the lesioned side had partly recovered at this time, it was still only $23 \pm 5\%$ of the activity in contralateral ganglia and $26 \pm 3\%$ of the activity in ganglia from the unoperated rats.

Delayed effects in spinal cord

The long-term depletion of ganglionic AChE and ChAT suggested that preganglionic sympathetic neurons might have degenerated after exposure to AChE antibody. The cell bodies of these cholinergic neurons were therefore examined by ChAT immunocytochemistry in the upper thoracic spinal cord. Samples were taken at one week, one month, and four months (three antibody-treated rats and three controls at each time). As expected, control samples showed clusters of ChAT-immunoreactive cell bodies in the IML nucleus at the T1–T2 level. Findings one

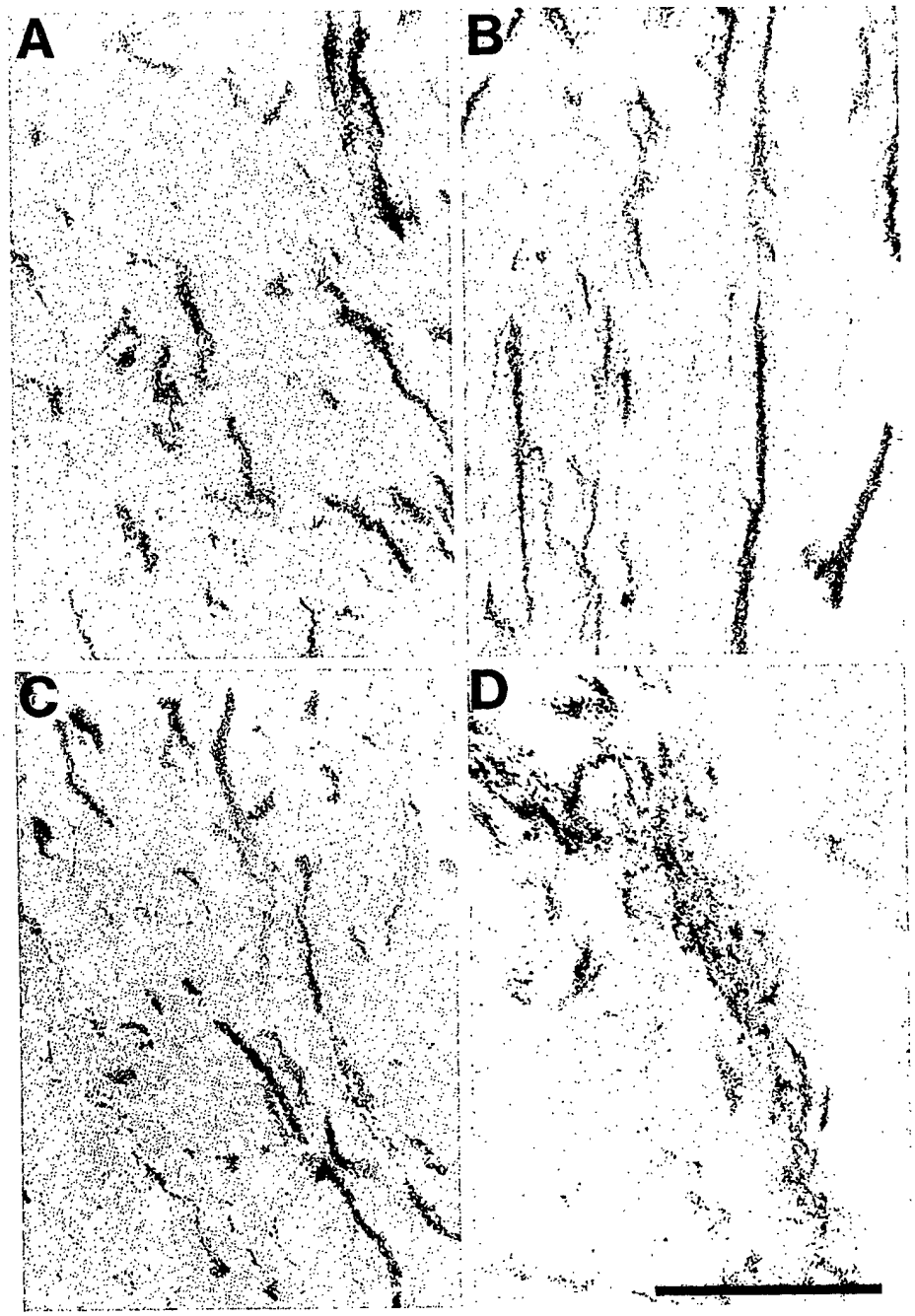

Fig. 11. Survival of terminal fibers in atrial musculature. AChE-staining by the method of Koelle and Friedenwald.[29] (A, B) Two control rats one week after i.v. injection of normal mouse IgG. (C, D) Two rats one week after i.v. injection of anti-AChE IgG. AChE-positive postganglionic parasympathetic fibers persist in the cardiac muscle tissue. Scale bar = 200 μm (all panels).

week after treatment with AChE-antibodies were similar (Fig. 15B). Four months after antibody treatment, however, the IML was structurally disorganized, ChAT-positive cell bodies were less abundant, and specific immunoreactivity in the neuropil was reduced (Fig. 15E). At the same time, ChAT-positive motor neurons in the adjacent ventral horn seemed to be unaffected (Fig. 15G). Quantitative morphometric analysis (Fig. 16) confirmed the impression that ChAT-positive neurons progressively disappeared from the thoracic IML (up to 70% loss, $P < 0.001$), while they remained undiminished in the ventral horn.

Because immunohistochemical deficits could reflect failure of ChAT expression rather than neuronal death, we also counted Nissl-stained neurons.

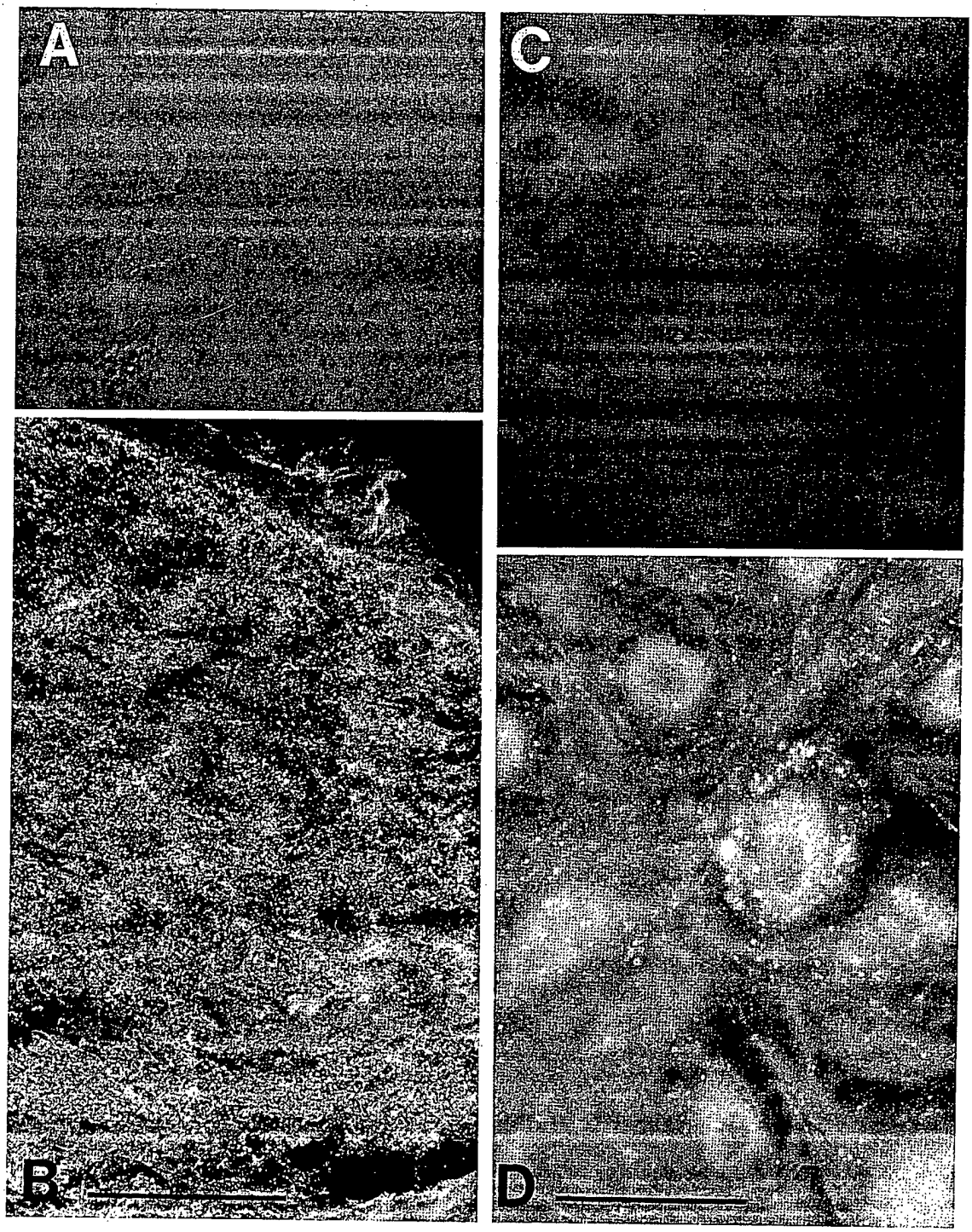

Fig. 12. Left: deposition of anti-AChE IgG in ganglia. Superior cervical ganglia stained for mouse IgG by direct immunofluorescence, 12 h after i.v. injection of normal mouse IgG (A) or anti-AChE IgG (B). Punctate immunofluorescence in B marks IgG deposits at AChE-rich, cholinergic synapses. Scale bar = 200 μm. Right: focal activation of complement in same ganglia. Complement component-C3 revealed by indirect immunofluorescence. Control ganglion (C) shows no specific staining. C3 Immunoreactivity in experimental ganglion (D) is localized to discrete punctate sites around periphery of perikarya and on dendrites in the neuropil. Scale bar = 50 μm.

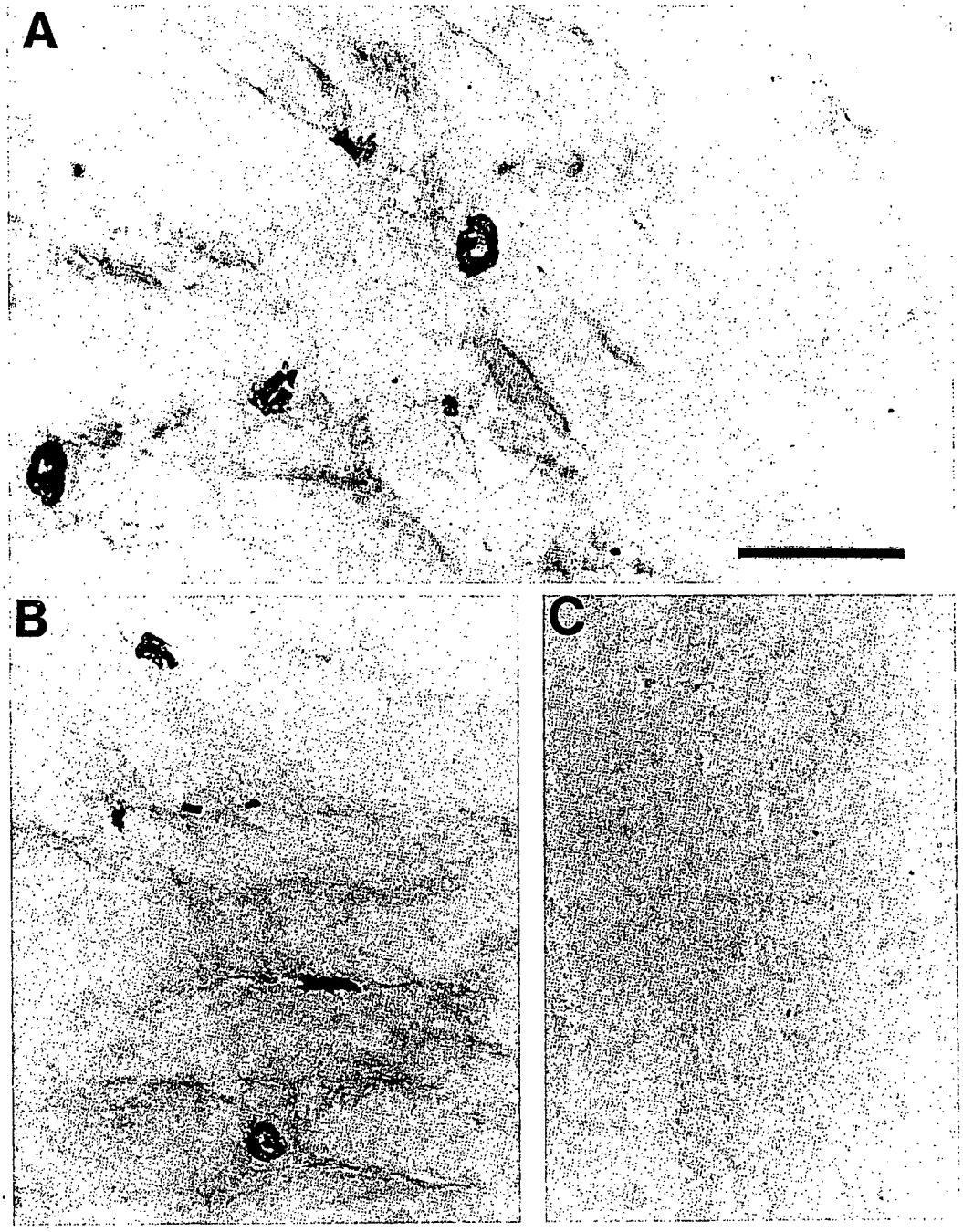

Fig. 13. Antibody access to neuromuscular junction. Diaphragm muscle stained for murine IgG by "ABC" peroxidase method. (A, B) Anti-AChE IgG injected i.v., 12 h earlier. Darkly stained, pretzel-shaped endplates were abundant. (C) Normal mouse IgG, injected i.v., 12 h earlier. Blank field representative of entire endplate-rich region. Scale bar = 100 μm.

Criteria defining the region and cells to be analysed (see Experimental Procedures) were chosen to minimize the chance of false-positive results. Accordingly we examined the entire IML region in each section of the T1–T2 cord, recognizing that some interneurons would be counted along with the preganglionic sympathetic neurons. A loss of cells after antibody treatment was evident by casual observation (Fig. 17), and was confirmed by systematic quantitation: the number of IML perikarya per section decreased from 23 ± 1.2 in controls ($n = 10$), to 13 ± 1.5 in the samples taken four months after antibody treatment ($n = 5$; $P < 0.001$). There were no obvious signs of chromatolysis in the surviving neurons.

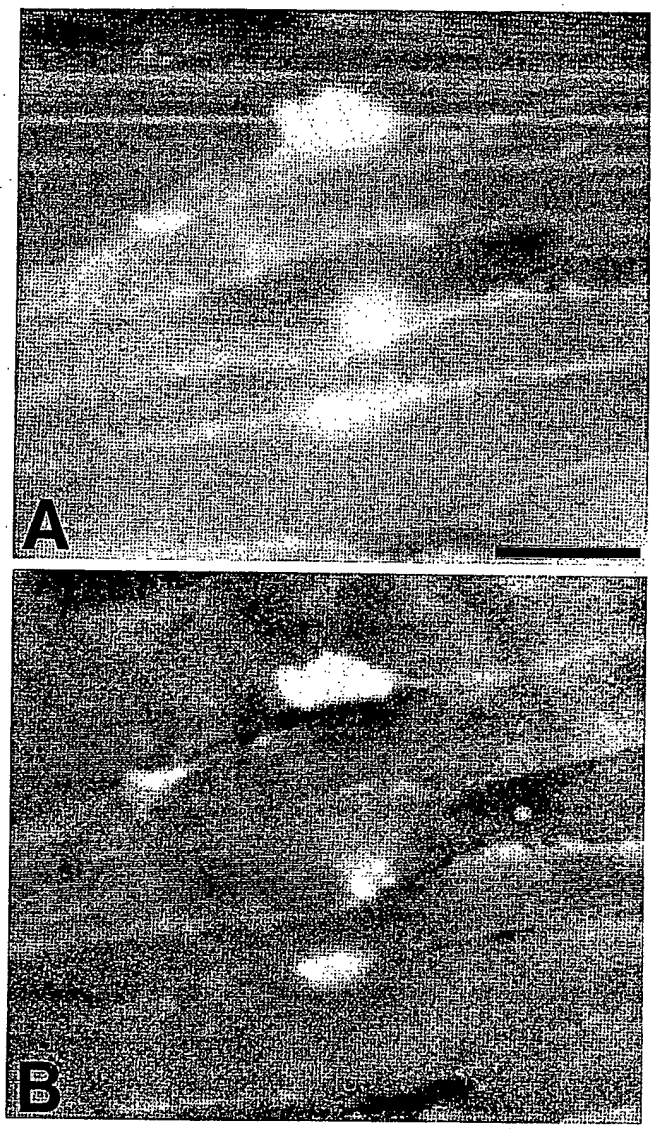

Fig. 14. Complement activation in neuromuscular junction. (A) Complement component-C3 visualized by indirect immunofluorescence 12 h after i.v. injection of anti-AChE IgG. (B) Endplate acetylcholine receptors identified by rhodamine-α-bungarotoxin binding (same slide). Video processing was used to enhance the fluorescence signal (see Experimental Procedures). The distributions of C3 and receptors match closely. Scale bar = 50 μm.

Spinal cords were also examined for GFAP, another indicator of neuronal damage. GFAP-immunoreactive astrocytes appeared abnormally abundant in IML specimens taken one month (three rats) and four months (one rat) after anti-AChE IgG (Fig. 18). Morphometry was not attempted, but the data indicated a moderate gliosis.

Fig. 15. Survival and loss of preganglionic sympathetic neurons in the intermediolateral cell column. Rats were given i.v. injections of normal mouse IgG (A, D, F) or anti-AChE IgG (B, E,G). Sections of the upper thoracic spinal cord (T1–T2 level) were stained for ChAT-immunoreactivity. Top row: IML nucleus, one week after injections. Note similar abundance of ChAT-immunoreactive IML neurons in A and B; C shows background staining in absence of specific first antibody. Middle row: IML nucleus, four months after injections. Note loss of ChAT immunoreactivity from neuropil and relative reduction in number of CHAT-positive perikarya in rat treated with anti-AChE IgG (E). Bottom row: ventral spinal cord, four months after injections. In control (F), ChAT-immunoreactive neurons are abundant in IML (arrow) and ventral horn. In anti-AChE IgG recipient (G), persistence of motor neurons in ventral horn contrasts with dearth of immunoreactive cells in IML (arrow). All scale bars = 100 μm.

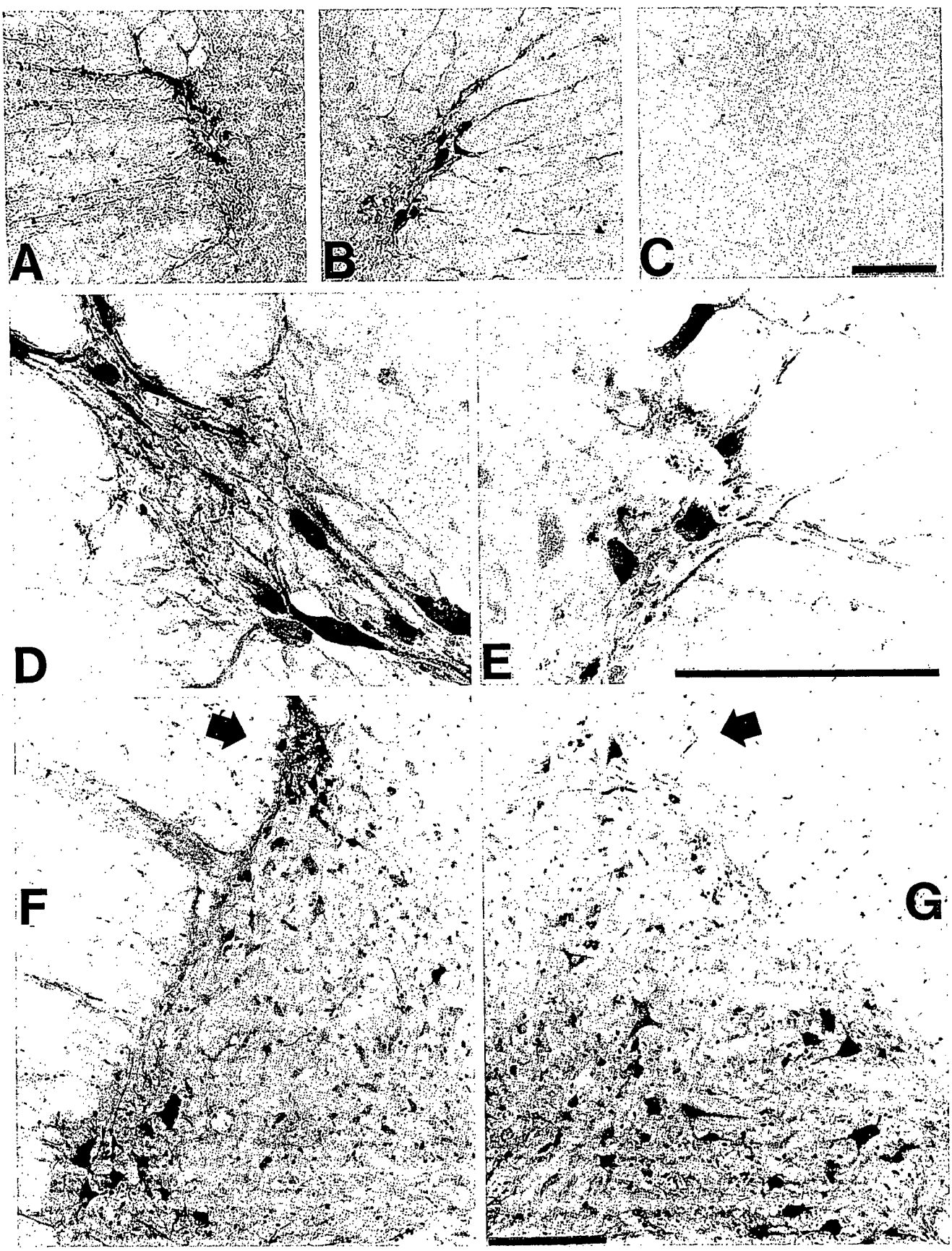

Fig. 15.

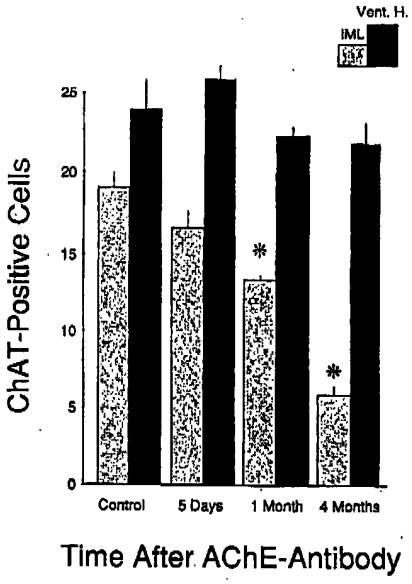

Fig. 16. Morphometric evidence for selective damage to preganglionic sympathetic perikarya. ChAT-positive neurons were counted under blinded conditions in the IML and ventral horn (Vent. H.). Samples were prepared at indicated times after IgG injection ($n = 3$ for each group receiving anti-AChE IgG; $n = 9$ for controls receiving normal mouse IgG). One-factor ANOVA showed a highly significant overall loss in the IML ($F = 21.1$ with 3 and 14 degrees of freedom, $P = 0.0001$). Asterisks indicate significant individual differences from control ($P < 0.01$).

DISCUSSION

Immunologic lesions focused on preganglionic sympathetic neurons

This study extends evidence that anti-AChE-antibodies selectively attack preganglionic sympathetic neurons[9] (see Table 2). Behavioral, biochemical and morphological data all indicate that the antibodies induce a nearly pure dysautonomia. We have shown that functional and biochemical deficits in some parts of the sympathoadrenal system are permanent, and we can now attribute this permanence to progressive death of preganglionic neuronal cell bodies in the spinal cord.

The behavioral data are consistent with a pathophysiological focus on the sympathetic nervous system, and they provide no evidence of a sensory or central neurological deficit. The only documented sign of motor dysfunction was weakness of grip, and this was remarkably mild in comparison with the profound sympathetic dysfunction. The modest long-term grip weakness may reflect a growth lag. Comparisons of grip-strength at similar body weights showed little difference between antibody-treated and control rats. Early grip weakness, on the other hand, could be a direct consequence of IgG binding to AChE in the neuromuscular junction. The immunocytochemical data support this view, as does the complexation of 16S AChE, an isoform believed to be synapse-specific.[22] Selective complexing of oligomeric forms with sparing of monomeric molecular forms would be predicted from the widely held model in which monomeric forms of AChE are primarily intracellular and oligomeric forms primarily extracellular.[19,57] However, it should be recognized that some of the IgG-bound AChE may have persisted in the muscle and retained its synaptic function, since the antibodies do not directly inhibit AChE activity. In any case, the acute biochemical effects of antibodies on synaptic forms of muscle AChE were transient. One can therefore infer that AChE antibodies do not damage motor neurons or endplates irreversibly.

Tissue-selective losses of ChAT paralleled the behavioral data even more closely than did changes in AChE. ChAT *per se* is not a target for AChE-antibodies but it is a highly specific cytoplasmic marker of cholinergic neurons.[14,55] The profound drop of ChAT activity in ganglia and adrenals therefore must reflect destruction of the cholinergic sympathoadrenal input.[9] Preservation of normal ChAT activity in muscle and heart, where it is a marker of motor and parasympathetic neurons, showed that those neurons resisted cytotoxic damage by AChE-antibodies. Thus, available information indicates that one class of AChE-bearing cell, the preganglionic sympathetic neuron, is selectively vulnerable to lesions by AChE-antibodies.

The exceptional vulnerability of preganglionic neurons would be easily understood if circulating anti-AChE IgG penetrated only sympathetic ganglia, not skeletal muscle or heart. However, selective access was unequivocally refuted by our finding of massive accumulations of AChE-specific IgG on antigenic targets in all types of cholinergic synapses. This finding, with our earlier demonstration that these antibodies recognize AChE *in vitro* from all tissues,[45] also rules out tissue-specific AChE epitopes as an explanation for tissue-selective damage.

Another potential mechanism for tissue selectivity would be recognition of a non-AChE antigen, uniquely expressed by preganglionic sympathetic neurons. We have not proven that each of our monoclonal antibodies recognizes AChE exclusively. However, the hypothesis of an alternative antigen is weakened by two facts: (i) The anti-AChE antibodies do not cause neural lesions when injected singly, only when given in combinations that recognize more than one AChE-epitope;[9] (ii) no single AChE-antibody is crucial to the efficacy of such antibody mixtures.[9] The reasonable interpretation is that AChE is the antigenic target in common, and that simultaneous occupation of multiple epitopes is needed to trigger the immunologic reactions that are pathogenic for nerve terminals.

Pathogenic role of immune complexes and complement

Initiation of neural lesions evidently begins with the formation of complexes between IgG and AChE exposed on cell surfaces throughout the peripheral

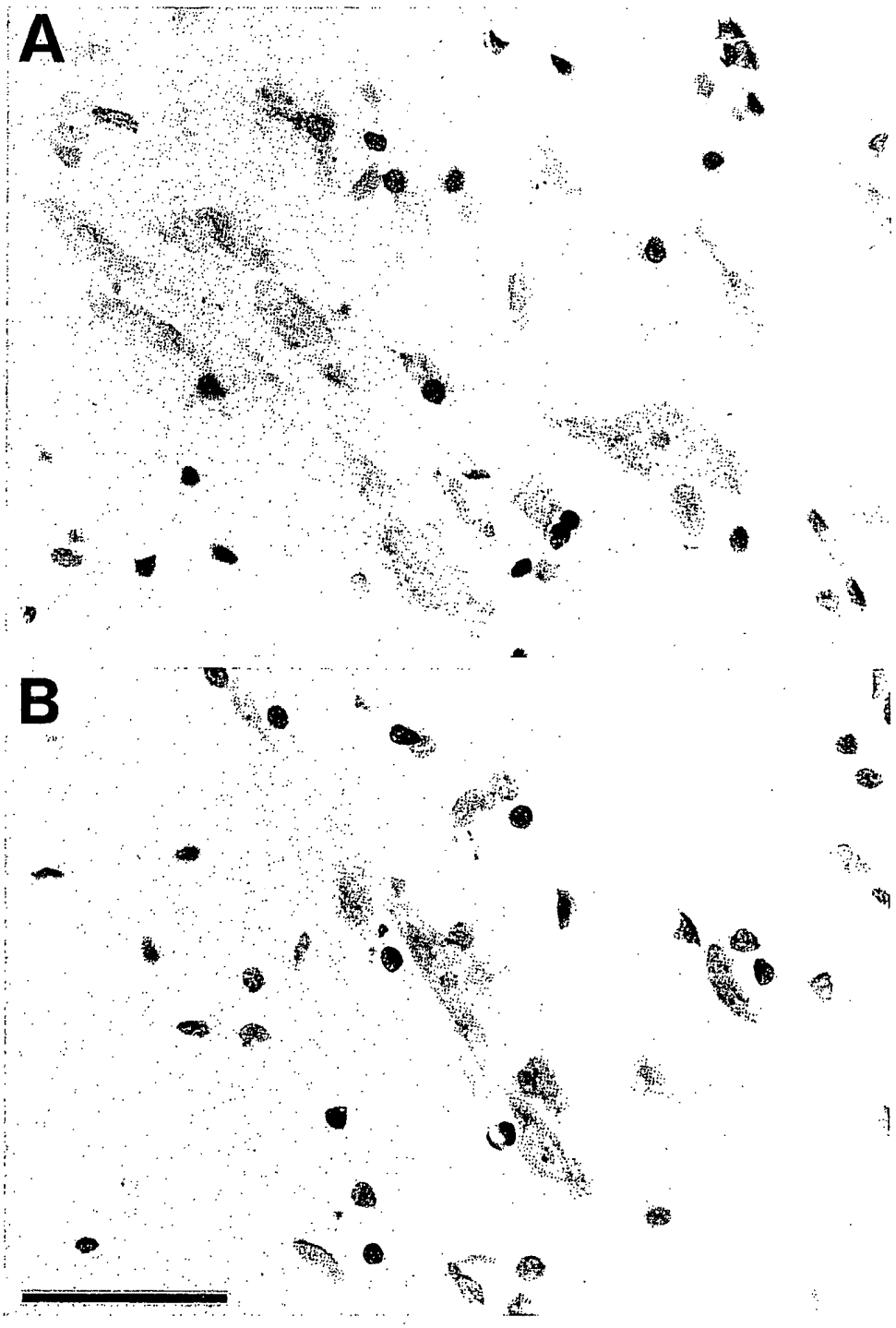

Fig. 17. Loss of Nissl-stained preganglionic sympathetic neurons. High power views of the IML nucleus at the T1–T2 level of the spinal cord, four months after i.v. injection of normal mouse IgG (A) or anti-AChE IgG (B). Small dark structures are glial nuclei. Scale bar = 50 μm. Note relative scarcity of neurons in B.

nervous system. The immunologic reactions that follow this step could be humoral, cellular, or a combination of both.

Cellular immunity may have a limited role in the neuropathology induced by AChE antibodies. T-cells would not be expected to play a major part in a passively transferred disorder. At times from 4 h to 90 days after antibody injection, inflammatory cells in ganglia were less numerous than one would anticipate in response to complement-mediated chemotactic

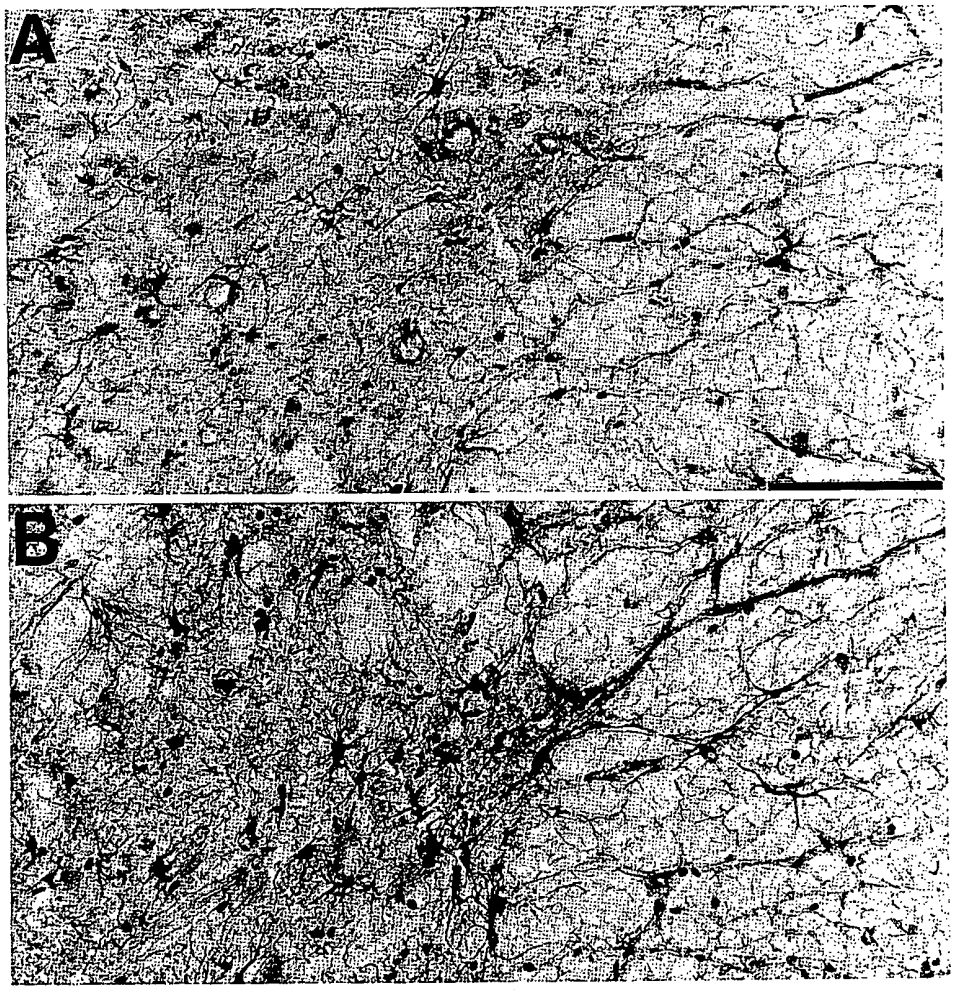

Fig. 18. Proliferation of GFAP-positive astrocytes in IML. Sections of spinal cord (T1–T2 level) were stained for GFAP four months after i.v. injection of normal mouse IgG (A) or anti-AChE IgG (B). Dark spidery cells are GFAP-positive astrocytes. Pale gray cells are Nissl-stained neurons. Scale bar = 100 μm.

Table 2. Selective neuropathology induced by antibodies to acetylcholinesterase

Effect	Evidence	Reference
Preganglionic sympathetic neurons damaged	Ptosis, miosis, hypotension, bradycardia	9
	No response to electrical stimulation of cervical sympathetic chain	9
	ChAT depleted from sympathetic ganglia and adrenal gland	9 and this article
	AChE lost from ganglionic neuropil	this article
	Ganglionic synapses degenerate and disappear	this article
	Intermediolateral spinal cord loses cholinergic perikarya	this article
Postganglionic adrenergic cells spared	Response to direct ganglionic stimulation persists	9
	Ganglia retain dopamine-β-hydroxylase activity	9
	Nissl-staining, AChE-positive neurons persist in ganglia	this article
	Tyrosine hydroxylase immunoreactivity persists in ganglionic neurons	unpublished
	Spleen, cardiac atria, adrenal glands and other adrenergic end organs retain near normal catecholamine content	unpublished
Somatic motor and parasympathetic systems largely spared	Motor function is normal (gait, reflexes) or near-normal (grip)	9 and this article
	Skeletal muscle retains acetylcholine receptors, endplates and ChAT	9 and this article
	Motor endplates have normal junctional folds	this article
	Spinal cord ventral horn retains cholinergic perikarya	this article
	Pupillary reflexes and negative chronotropic vagal responses persist	9 and this article
	Cardiac atria retain ChAT activity	9 and this article
	Atrial muscle retains AChE-positive nerve fibers	this article
	Atrial ganglia retain AChE-positive neurons; some fibers lost	this article

signals. The few macrophages and leukocytes that did appear were probably involved in secondary reactions to complement-induced injury of ganglionic terminals, analogous to the Wallerian degeneration of transected peripheral nerve.[3,40]

There are precedents for complement-mediated lysis of nerve terminals opsonized by a specific antibody *in vitro*.[15,43,44,51] Closer to our *in vivo* paradigm is the adrenergic pathology in guinea-pigs given antiserum to dopamine-β-hydroxylase, i.v. Studies with this model found widespread degeneration of adrenergic terminals except at sites where complement was limited.[13,21,48] In our previous work with AChE antibodies,[9] we were able to prevent sympathetic deficits by depleting complement with cobra venom factor.[4] Clearly, complement must be activated in order for AChE-antibodies to cause neural damage. However, the results do not explain why most cholinergic cells escape detectable damage. Our immunocytochemical data reveal that complement is extensively activated in muscle and heart as well as sympathetic ganglia. This implies that the target cells in muscle and heart may be intrinsically resistant to the cytotoxic sequelae.

Resistance to complement is not surprising, since nucleated cells generally survive a combined assault by antibody and complement.[50,56] Survival may be influenced by surface–volume ratios, which favor compact structures over finely branched synaptic terminals. For example, adrenal chromaffin cells resisted the dopamine-β-hydroxylase antiserum that lysed adrenergic nerve terminals.[21,48] Similarly, when our AChE-antibodies were injected into the rat striatum, AChE-rich perikarya survived although cholinergic terminals were devastated.[6]

Neuronal perikarya, adrenal cells and myocytes all have low surface–volume ratios that should minimize the consequences of membrane damage. Yet surface–volume ratios are high at most nerve endings, while AChE antibodies preferentially destroy preganglionic sympathetic terminals. Hence, additional factors probably serve to determine vulnerability to antibody and complement. We previously speculated[9] that motor nerve endings and muscle membranes are protected by the large store of asymmetric AChE in the synaptic basal lamina,[26,33,34] which may form a trap for AChE-antibodies and activated complement. Sympathetic ganglia lack a comparable feature. Extracellular trapping is a testable hypothesis to account for the unique specificity of neuronal lesions by AChE-antibodies. Other possibilities for investigation include the different cell-specific modes by which AChE is anchored to synaptic surface membranes.

Death of spinal neurons explains permanent dysautonomia

A hallmark of the sympathectomy induced by AChE-antibodies is its permanence, which contrasts sharply with the reversibility of damage caused by crush injury. This can only be understood in relation to events in the spinal cord, the site of preganglionic neuronal cell bodies. There we documented a selective loss of cholinergic perikarya in the upper thoracic portion of the intermediolateral column, with no discernible effects on cholinergic neurons in the ventral horn. Sparing of the ventral horn neurons was expected, in the face of functional and biochemical integrity in the somatic motor system. On the other hand, we did not anticipate cell death in the intermediolateral column, despite the extensive lesions of cholinergic terminals in the sympathetic ganglia.

One would expect nerve terminals to be repaired readily after damage by AChE-antibodies, just as motor endplates are repaired after damage by exogenous anti-nicotinic receptor-antibodies.[49] Nonetheless, the delayed disappearance of ChAT-positive and Nissl-stained preganglionic neurons at the T1–T2 level of the spinal cord implies that these cells succumbed to the peripheral lesion induced by anti-AChE antibody and complement. This observation plausibly accounts for the long-lasting functional and biochemical deficits in the ganglia.

Neuronal death in the IML appears to have been accompanied by a reactive astrocytosis as evidenced by proliferation of GFAP-staining cells, albeit modest in comparison with lesions induced by neurotoxic heavy metals.[38] The differing intensity of the glial reactions may reflect a difference in the site of the primary cellular damage.

It is unlikely that cholinergic neurons in the IML were destroyed by AChE antibodies penetrating the spinal cord. We have documented elsewhere that these IgGs do not accumulate in the CNS except in newborn animals.[8,46] Neuronal death in the IML must be a response to the complement-mediated destruction of preganglionic terminals in the periphery. It is recognized that sensory neurons can die weeks or months after axonal transection.[2,12,24,32] but sympathetic neurons often regenerate after traumatic injury. For example, postganglionic adrenergic neurons typically die after ligation of efferent fibers, but they recover from crush injury at the same locus.[41] Preganglionic neurons also regenerate, for example, after the input to the cat superior cervical ganglion is severed.[42] However, not all preganglionic neurons necessarily survive an injury. In the rat we observed slow return of eyelid tone after crushing the cervical sympathetic chain, yet the superior cervical ganglia regained only a fraction of their previous ChAT activity. This finding is consistent with a partial depopulation of the IML.

Presumably, central perikarya are at risk of degenerating if they lose their peripheral contacts. Contributing factors might include deprivation of trophic factors[1,23] or receipt of "chromatolytic signals"[7] transported from the truncated distal processes. Thus, a common mechanism could cause neuronal death after immunologic and mechanical disruption of terminals. However, there seems to be

no precedent for the extensive, delayed loss of central perikarya that follows the peripheral lesions induced by anti-AChE IgG and complement. Conceivably, AChE antibodies exert additional pathologic effects by virtue of uptake at nerve terminals and retrograde transport back to cell bodies. This remains to be established. It is also not known whether preganglionic neurons are affected equally at all levels of the spinal cord or whether function is impaired to a uniform extent throughout the sympathetic system. A detailed survey of the regional cellular binding of antibodies, the neuropathology of prevertebral ganglia and lumbar cord, and the transcriptional responses of neuronal cell bodies may shed light on these issues.

Acknowledgements—This work was supported by grants NS18170, NS29646, and NS23537 from the National Institutes of Health. Aid with injections and tissue preparation was provided by Dr Stephanie Padilla, Neurotoxicology Branch, U.S.E.P.A. Health Effects Laboratory, Research Triangle Park NC.

REFERENCES

1. Angeletti P. U., Levi-Montalcini R. and Caramia F. (1971) Analysis of the antiserum to the nerve growth factor in adult mice. *Brain Res.* **27**, 343–355.
2. Arvidsson J., Ygge J. and Grant G. (1986) Cell loss in lumbar dorsal root ganglia and transganglionic degeneration after sciatic nerve resection in the rat. *Brain Res.* **373**, 15–21.
3. Asbury A. K. (1982) Peripheral nerves. In *Histopathology of the Nervous System* (eds W. Haymaker and R. D. Adams), pp. 1566–1610. Thomas, Springfield.
4. Ballow M. and Cochrane C. G. (1969) Two anticomplementary factors in cobra venom: hemolysis of guinea pig erythrocytes by one of them. *J. Immunol.* **103**, 944–952.
5. Barber R. P., Phelps P. E., Houser C. R., Crawford G. D., Salvaterra P. M. and Vaughn J. E. (1984) The morphology and distribution of neurons containing choline acetyltransferase in the adult rat spinal cord: an immunocytochemical study. *J. comp. Neurol.*
6. Bean A. J., Zhang X., Brimijoin S. and Hökfelt T. (1991) Effect of intracerebral injection of monoclonal acetylcholinesterase antibodies on cholinergic nerve terminals in the rat central nervous system. *Neurosci. Lett.* **133**, 145–149.
7. Bisby M. and Bulger V. T. (1977) Reversal of axonal transport at a nerve crush. *J. Neurochem.* **29**, 313–320.
8. Brimijoin S., Balm M., Hammond P. and Lennon V. A. (1990) Selective complexing of acetylcholinesterase in brain by intravenously administered monoclonal antibody. *J. Neurochem.* **54**, 236–241.
9. Brimijoin S. and Lennon V. A. (1990) Autoimmune preganglionic sympathectomy induced by acetylcholinesterase antibodies. *Proc. natn. Acad. Sci.* **87**, 9630–9634.
10. Brimijoin S., Skau K. A. and Wiermaa M. J. (1978) On the origin and fate of external acetylcholinesterase in peripheral nerve. *J. Physiol., Lond.* **285**, 143–158.
11. Bruck C., Portetelle D., Glineur C. and Bollen A. (1982) One-step purification of mouse monoclonal antibodies from ascites fluid by DEAE Affi-Gel Blue chromatography. *J. immun. Meth.* **53**, 313–319.
12. Cavanaugh M. W. (1951). Quantitative effects of the peripheral innervation area on nerves and spinal ganglion cells. *J. comp. Neurol.* **94**, 181–219.
13. Costa M., Rush R. A., Furness J. B. and Geffen L. B. (1976) Histochemical evidence for degeneration of peripheral noradrenergic axons following intravenous injection of antibodies to dopamine-β-hydroxylase. *Neurosci. Lett.* **3**, 201–207.
14. Cuello A. C. and Sofroniew M. V. (1984) The anatomy of the CNS cholinergic neurons. *Trends Neurosci.* **7**, 74–78.
15. Docherty M., Bradford H. and Anderton B. (1982) Lysis of cholinergic synaptosomes by an antiserum to choline acetyltransferase. *Fedn Eur. biochem. Socs Lett.* **144**, 47–50.
16. Donovick P. (1974) A metachromatic stain for neural tissue. *Stain Technol.* **49**, 49–51.
17. Eckenstein F., Thoenen H. (1982) Production of specific antisera and monoclonal antibodies to choline acetyltransferase: characterization and use for identification of cholinergic neurons. *Eur. molec. Biol. Org. J.* **1**, 363–368.
18. Ellman G. L., Courtney K. D., Andres V. Jr and Featherstone R. M. (1961) A new and rapid colorimetric determination of acetylcholinesterase activity. *Biochem. Pharmac.* **7**, 88–95.
19. Fernandez H. L., Duell M. J. and Festoff B. W. (1979) Cellular distribution of 16S acetylcholinesterase. *J. Neurochem.* **32**, 581–585.
20. Fonnum F. (1975) A rapid radiochemical method for the determination of choline acetyltransferase. *J. Neurochem.* **24**, 407–409.
21. Furness J. B., Lewis S. Y., Rush R., Costa M. and Geffen L. B. (1977) Involvement of complement in degeneration of sympathetic nerves after administration of DBH antibodies. *Brain Res.* **136**, 67–75.
22. Hall Z. W. (1973) Multiple forms of acetylcholinesterase and their distribution in endplate and non-endplate regions of rat diaphragm muscle. *J. Neurobiol.* **4**, 343–361.
23. Hendry I. A., Stoeckel K., Thoenen H. and Iversen L. L. (1974) The retrograde axonal transport of nerve growth factor. *Brain Res.* **68**, 103–121.
24. Himes B. T. and Tessler A. (1989) Death of some dorsal root ganglion neurons and plasticity of others following sciatic nerve section in adult and neonatal rats. *J. comp. Neurol.* **284**, 215–230.
25. Hsu S. M., Raine L. and Fanger H. (1981) Use of avidin–biotin–peroxidase complex (ABC) in immunoperoxidase techniques: a comparison between ABC and unlabelled antibody (PAP) procedures. *J. Histochem. Cytochem.* **29**, 577–580.
26. Inestrosa N. C., Silberstein L. and Hall Z. W. (1982) Association of the synaptic form of acetylcholinesterase with extracellular matrix in cultured mouse muscle cells. *Cell* **29**, 71–79.
27. Johnson C. D. and Russell R. L. (1975) A rapid and simple radiometric assay for cholinesterase, suitable for multiple determinations. *Analyt. Biochem.* **64**, 229–238.

28. Kiernan J. A. (1980) *Histological and Histochemical Methods. Theory and Practice*, pp. 162–163. Pergamon Press, Oxford.
29. Koelle G. B. and Friedenwald J. S. (1949) A histochemical method for localizing cholinesterase activity. *Proc. Soc. exp. Biol. Med.* **70**, 617–622.
30. Lennon V. A. and Lambert E. H. (1989) Autoantibodies bind solubilized calcium channel-ω-conotoxin complexes from small cell lung carcinoma: a diagnostic aid for Lambert–Eaton myasthenic syndrome. *Mayo Clin. Proc.* **64**, 1498–1504.
31. Lennon V. A., Lindstrom J. M. and Seybold M. E. (1976) Experimental autoimmune myasthenia gravis: cellular and humoral immune responses. *Ann. N.Y. Acad. Sci.* **274**, 283–299.
32. Lieberman A. R. (1971) The axon reaction: a review of the principal features of perikaryal responses to axon injury. *Int. Rev. Neurobiol.* **14**, 49–124.
33. Marshall L. M., Sanes J. R. and McMahan U. J. (1977) Reinnervation of original synaptic sites on muscle fiber basement membrane after disruption of the muscle cells. *Proc. natn. Acad. Sci.* **74**, 3073–3077.
34. McMahan U. J., Sanes J. R. and Marshall L. M. (1978) Cholinesterase is associated with the basal lamina at the neuromuscular junction. *Nature* **271**, 172–174.
35. Momoi M. Y. and Lennon V. A. (1982) Purification and biochemical characterization of nicotinic acetylcholine receptors of human muscle. *J. biol. Chem.* **257**, 12,757–12,764.
36. Moser V. C. (1991) Investigations of amitraz neurotoxicity in rats. IV. Assessment of toxicity syndrome using a functional observational battery. *Fundam. appl. Toxic.* **17**, 7–16.
37. Moser V. C., McCormick J. P., Creason V. P. and MacPhail R. C. (1988) Comparison of chlordimeform and carbaryl using a functional observational battery. *Fundam. appl. Toxic.* **11**, 189–206.
38. O'Callaghan J. P. and Miller D. B. (1983) Nervous system-specific proteins as biochemical indicators of neurotoxicity. *Trends pharmac. Sci.* **4**, 388–390.
39. Patrick J. and Lindstrom J. (1973) Autoimmune response to acetylcholine receptor. *Science* **180**, 871–872.
40. Perry V. H., Hume D. A. and Gordon S. (1985) Immunohistochemical localization of macrophages and microglia in the adult and developing mouse brain. *Neuroscience* **15**, 313–326.
41. Purves D. (1975) Functional and structural changes in mammalian sympathetic neurones following interruption of their axons. *J. Physiol.* **252**, 429–463.
42. Raisman G., Field P. M., Ostberg A., Iversen L. L. and Zigmond R. E. (1974) A quantitative ultrastructural and biochemical analysis of the process of reinnervation of the superior cervical ganglion of the adult rat. *Brain Res.* **71**, 1–17.
43. Raiteri M., Bertollini A. and La Bella R. (1972) Synaptosome antisera affect permeability of synaptosomal membranes *in vitro*. *Nature New Biol.* **238**, 242–243.
44. Raiteri M. and Levi G. (1973) Antisynaptosome antibodies affect synaptosomal permeability to neurotransmitters. *Nature New Biol.* **245**, 89–91.
45. Rakonczay Z. and Brimijoin S. (1986) Monoclonal antibodies to rat brain acetylcholinesterase: comparative affinity for soluble and membrane-associated enzyme and for enzyme from different vertebrate species. *J. Neurochem.* **46**, 280–287.
46. Rakonczay Z., Hammond P. and Brimijoin S. (1993) Lesion of central cholinergic systems by systemically administered acetylcholinesterase antibodies in newborn rats. *Neuroscience* **54**, 225–238.
47. Rando T. A., Bowers C. W. and Zigmond R. E. (1981) Localization of neurons in the rat spinal cord which project to the superior cervical ganglion. *J. comp. Neurol.* **196**, 73–83.
48. Rush R. A., Costa M., Furness J. B. and Geffen L. B. (1976) Changes in tyrosine hydroxylase and dopamine-β-hydroxylase activities during degeneration of noradrenergic axons produced by antibodies to dopamine-β-hydroxylase. *Neurosci. Lett.* **3**, 209–213.
49. Sahashi K., Engel A. G., Lindstrom J. M., Lambert E. H. and Lennon V. A. (1978) Ultrastructural localization of immune complexes (IgG and C3) at the end-plate in experimental autoimmune myasthenia gravis. *J. Neuropath. exp. Neurol.* **37**, 212–223.
50. Schwartz R. S. and Datta S. K. (1989) Autoimmunity and autoimmune diseases. In *Fundamental Immunology* (ed. Paul W. E.), pp. 819–866. Raven Press, New York.
51. Schweitzer E. S. and Blaustein M. P. (1980) The use of antibody and complement to gain access to the interior of presynaptic nerve terminals. *Expl Brain Res.* **38**, 443–453.
52. Strack A. M., Sawyer W. B., Marubio L. M. and Loewy A. D. (1988) Spinal origin of sympathetic preganglionic neurons in the rat. *Brain Res.* **455**, 187–191.
53. Tago H., Kimura H. and Maeda T. (1986) Visualization of detailed acetylcholinesterase fiber and neuron staining in rat brain by a sensitive histochemical procedure. *J. Histochem. Cytochem.* **34**, 1431–1438.
54. Toyka K. V., Drachman D. B., Pestronk A. and Kao I. (1975) Myasthenia gravis: passive transfer from man to mouse. *Science* **190**, 397–399.
55. Tucek S. (1990) The synthesis of acetylcholine: twenty years of progress. *Prog. Brain Res.* **84**, 467–477.
56. Young J. D. and Cohn Z. A. (1987) Cellular and humoral mechanisms of cytotoxicity: Structural and functional analogies. *Adv. Immunol.* **41**, 269–332.
57. Younkin S. G., Rosenstein C., Collins P. L. and Rosenberry T. L. (1982) Cellular localization of the molecular forms of acetylcholinesterase in rat diaphragm. *J. biol. Chem.* **257**, 13,630–13,637.

(*Accepted* 2 *December* 1992)